Terminal Ordovician carbon isotope stratigraphy and glacioeustatic sea-level change across Anticosti Island (Québec, Canada)

David S. Jones[1,†], David A. Fike[1], Seth Finnegan[2], Woodward W. Fischer[2], Daniel P. Schrag[3], and Dwight McCay[1]
[1]*Department of Earth and Planetary Sciences, Washington University in St. Louis, 1 Brookings Drive, St. Louis, Missouri 63130, USA*
[2]*Division of Geological and Planetary Sciences, California Institute of Technology, 1200 East California Boulevard, MC 100-23, Pasadena, California 91125, USA*
[3]*Department of Earth and Planetary Sciences, Harvard University, 20 Oxford Street, Cambridge, Massachusetts 02138, USA*

ABSTRACT

Globally documented carbon isotope excursions provide time-varying signals that can be used for high-resolution stratigraphic correlation. We report detailed inorganic and organic carbon isotope curves from carbonate rocks of the Ellis Bay and Becscie Formations spanning the Ordovician-Silurian boundary on Anticosti Island, Québec, Canada. Strata of the Anticosti Basin record the development of a storm-dominated tropical carbonate ramp. These strata host the well-known Hirnantian positive carbon isotope excursion, which attains maximum values of ~4.5‰ in carbonate carbon of the Laframboise Member or the Fox Point Member of the Becscie Formation. The excursion also occurs in organic carbon, and $\delta^{13}C_{carb}$ and $\delta^{13}C_{org}$ values covary such that no reproducible $\Delta^{13}C$ (= $\delta^{13}C_{carb} - \delta^{13}C_{org}$) excursion is observed. The most complete stratigraphic section, at Laframboise Point in the west, shows the characteristic shape of the Hirnantian Stage excursion at the global stratotype section and point (GSSP) for the Hirnantian Stage in China and the Silurian System in Scotland. We therefore suggest that the entire Hirnantian Stage on Anticosti Island is confined to the Laframboise and lower Fox Point Members.

By documenting discontinuities in the architecture of the carbon isotope curve at multiple stratigraphic sections spanning a proximal to distal transect across the sedimentary basin, we are able to reconstruct glacioeustatic sea-level fluctuations corresponding to maximum glacial conditions associated with the end-Ordovician ice age. The combined litho- and chemostratigraphic approach provides evidence for the diachroneity of the oncolite bed and Becscie limestones; the former transgresses from west to east, and the latter prograde from east to west. The sea-level curve consistent with our sequence-stratigraphic model indicates that glacioeustatic sea-level changes and the positive carbon isotope excursion were not perfectly coupled. Although the start of the isotope excursion and the initial sea-level drawdown were coincident, the peak of the isotope excursion did not occur until after sea level had begun to rise. Carbon isotope values did not return to baseline until well after the Anticosti ramp was reflooded. The sea-level–$\delta^{13}C_{carb}$ relationship proposed here is consistent with the "weathering" hypothesis for the origin of the Hirnantian $\delta^{13}C_{carb}$ excursion.

INTRODUCTION

One of the largest mass extinctions of the Phanerozoic took place at the close of the Ordovician Period (Sepkoski, 1981; Brenchley et al., 2001; Sheehan, 2001; Bambach et al., 2004), an interval also marked by the development of extensive continental ice sheets on the south polar supercontinent Gondwana (Hambrey and Harland, 1981; Hambrey, 1985; Ghienne, 2003; Le Heron et al., 2007; Le Heron and Dowdeswell, 2009; Le Heron and Howard, 2010; Loi et al., 2010). This glaciation and the possible Early Silurian glaciation (Caputo and Crowell, 1985; Grahn and Caputo, 1992; Díaz-Martínez and Grahn, 2007) stand out as the only episodes in a 210 m.y. stretch (ca. 580–370 Ma) that otherwise lacks direct geologic evidence for continental ice sheets (Hambrey and Harland, 1981). This interval is thought to have occurred in a greenhouse interval dominated by high atmospheric pCO$_2$ (e.g., Berner, 2006), although sedimentary records of shoreline ice in tropical Laurentia in Middle to Late Cambrian time complicate this picture (Runkel et al., 2010). The biological crisis that accompanied the glaciation was the second greatest mass extinction in the marine fossil record (Sheehan, 2001; Bambach et al., 2004), depleting the enormous diversity of marine organisms that had evolved during the Ordovician Radiation (Webby et al., 2004). Marine carbonate rocks deposited at the time preserve records of a global disturbance to the carbon cycle represented by positive excursions in $\delta^{13}C_{carb}$ and $\delta^{13}C_{org}$ (Marshall and Middleton, 1990; Brenchley et al., 1994; Underwood et al., 1997; Wang et al., 1997; Ripperdan et al., 1998; Kump et al., 1999). Some of the sedimentary records also host geochemical evidence of global cooling and/or ice-sheet growth represented by parallel positive excursions in $\delta^{18}O_{carb}$ (Marshall and Middleton, 1990; Long, 1993; Brenchley et al., 2003).

Although much progress has been made in end-Ordovician correlation and carbon isotope chemostratigraphy (Finney et al., 1999; Kump et al., 1999; Brenchley et al., 2003; Melchin and Holmden, 2006; Kaljo et al., 2008; LaPorte et al., 2009; Yan et al., 2009; Zhang et al., 2009; Ainsaar et al., 2010; Desrochers et al., 2010; Young et al., 2010), uncertainty remains about the causal relationship among glaciation, mass extinction, and perturbation to the carbon cycle. Delabroye and Vecoli (2010) recently reviewed some of the outstanding issues in Hirnantian event stratigraphy, emphasizing shortcomings in the current biostratigraphic and chemostratigraphic correlations. Although many pieces of evidence suggest that the glaciation, extinction, and geochemical disturbance were synchronous (Marshall and Middleton, 1990; Long, 1993; Brenchley and Marshall, 1999; Brenchley et al., 2003), no sedimentary succession contains well-preserved records of all three events.

Without a firm chronological framework, it is difficult to make strong statements regarding the causes, consequences, and interrelatedness of the events.

†Current address: Department of Geology, Amherst College, 11 Barrett Hill Road, Amherst, Massachusetts 01002, USA; djones@amherst.edu

In this paper, we present new high-resolution stable isotope data coupled to lithostratigraphy from the Lousy Cove and Laframboise Members of the upper Ellis Bay Formation and the Fox Point Member of the lower Becscie Formation on Anticosti Island in eastern Canada (Fig. 1). Because the carbon isotopic composition of the global ocean changes smoothly (rather than discontinuously) in time, carbon isotope excursions can provide time-varying signals that allow for high-resolution stratigraphic correlation. Brenchley et al. (2003) used the Hirnantian positive carbon isotope excursion to achieve high-resolution intrabasinal correlations within Baltica, and interbasinal correlation between Baltica and Laurentia, improving our understanding of the relative timing of environmental changes, isotopic evolution, and biotic events associated with the end-Ordovician extinction and glaciation. In this paper, we employ the Hirnantian positive carbon isotope excursion for high-resolution intrabasinal correlation within the Anticosti Basin. By documenting the relationships between discontinuities in the chemostratigraphic record and disconformities in the lithostratigraphic record, we can construct a new sequence-stratigraphic model for glacio-eustatic sea-level fluctuations associated with end-Ordovician Earth history.

Geological Setting

The autochthonous Ordovician–Silurian Anticosti Basin was deposited on top of Grenville-age crust on the eastern margin of Laurentia (Waldron et al., 1998). Sedimentation in the basin began in the latest Cambrian as the region experienced waning effects of the thermal subsidence (Waldron et al., 1998) that began in the Ediacaran Period around 615 Ma (Kamo and Gower, 1994). In Middle Ordovician time, the advance of the Taconic arc from the south and east reinvigorated flagging subsidence rates (Waldron et al., 1998; Long, 2007). Back-stripping analysis using ages and water depths inferred from paleontological data suggests an increase in sedimentation rate as the foreland basin developed through the Sandbian and Katian Stages of the Ordovician (Long, 2007). Sediments continued to accumulate during the Early Silurian, but deposition waned once Taconic thrust loading ended in the Llandovery (Long, 2007), diminishing the production of additional accommodation space. Thermal maturation data, basin modeling, and offshore seismic data demonstrate that Anticosti strata were subsequently buried no deeper than 2.5–3 km and are still in the oil window (Pinet and Lavoie, 2007). There has been little significant structural deformation to the island, although structural analysis indicates the presence of fracture sets produced by Taconic, Acadian, and/or Jurassic events (Bordet et al., 2010).

Although over 3 km of sediment accumulated in the Upper Ordovician–Lower Silurian Anticosti Basin, over two-thirds of the succession is known only from subsurface exploration (INRS-Petrole, 1974). The Romaine, Mingan, Trenton–Black River, Macasty, and Princeton Lake Formations have been characterized through borehole sampling (INRS-Petrole, 1974). The lower Vauréal Formation is also confined to the subsurface, but its upper ~300 m crop out on the surface (Long and Copper, 1987a). It has been subdivided into the informal La Vache, Easton, Tower, Homard, and Joseph Point members, and the formal Mill Bay and Schmitt Creek Members (Long, 2007). The Vauréal is succeeded by the Ellis Bay Formation, which has been divided into the Grindstone, Velleda, Prinsta, Lousy Cove, and Laframboise Members (Fig. 2A) (Long and Copper, 1987a). The Lower Silurian Becscie Formation overlies the Ellis Bay; it is composed of the Fox Point and Chabot Members (Copper and Long, 1989; Sami and Desrochers, 1992; Long, 2007). The remainder of the Anticosti succession includes the Merrimack, Gun River, Jupiter, and Chicotte Formations (Fig. 2B). This paper focuses on strata of the Lousy Cove, Laframboise, and Fox Point Members.

Most workers have interpreted the Anticosti Basin sedimentary record to represent a subtidal, storm-influenced, carbonate ramp-platform (Long and Copper, 1987a; Sami and Desrochers, 1992; Farley and Desrochers, 2007; Long, 2007; Desrochers et al., 2010). The long axis of the island is oblique to the paleoshoreline, with the east end occupying a more proximal position and the west end occupying a more distal position. Previous stratigraphic work has established several cycles of glacioeustatic sea-level fluctuation in the Vauréal and Ellis Bay Formations, argued to have been caused by the waxing and waning of continental ice sheets on Gondwana (Desrochers et al., 2010).

Chemostratigraphic Records across the Ordovician-Silurian Boundary

The global boundary stratotype section and point (GSSP) for the Hirnantian Stage is at Wangjiawan, North China, where it coincides

Figure 1. Geologic map of Anticosti Island, modified from Desrochers and Gauthier (2009), showing locations of studied sections. Approximately 900 m of gently dipping Ordovician to Silurian stratigraphy are exposed on the island. The Laframboise Member of the Ellis Bay Formation is the main target of this work. It is the uppermost member of the Ellis Bay Formation, occurring just below the Ellis Bay–Becscie contact. Facies associations may be grouped into the western sector (west coast and sections near Laframboise Point: sections D801–D806, D821, 901), east-central sector (Natiscotec River tributary: section 920; Salmon River: sections D814, D816, D817, 908, 909, 911; and Macaire Creek: D813, D815, 912), and eastern sector (Lousy Cove to Fox Point: section 914).
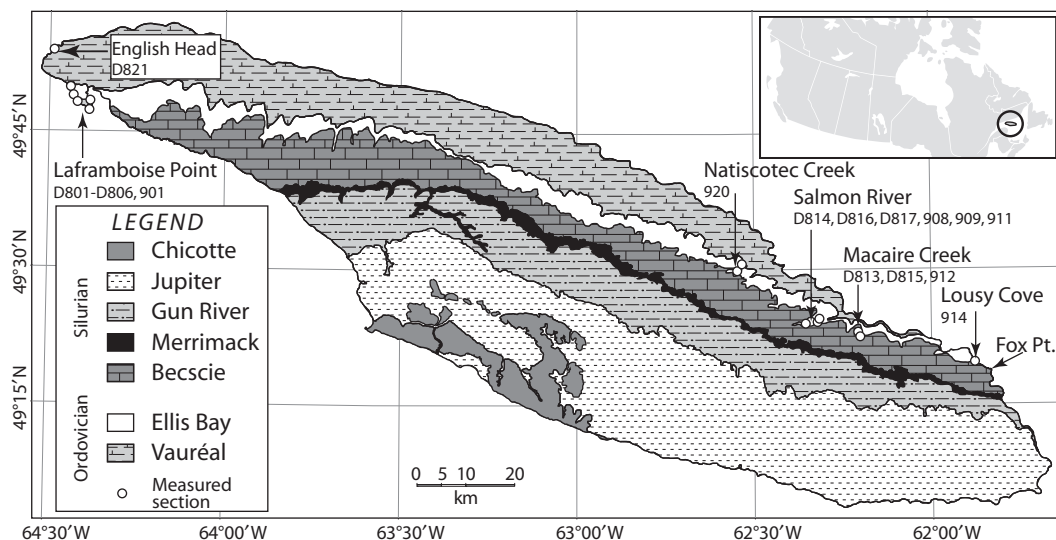
with the first appearance of the graptolite *Normalograptus extraordinarius* (Chen et al., 2006). The δ¹³C$_{org}$ record of a parallel section 180 m to the southeast of the GSSP, Wangjiawan Riverside (Chen et al., 2006), hosts a prominent positive δ¹³C$_{org}$ excursion in Hirnantian strata (Fig. 3). At this location, the pre-excursion

δ¹³C$_{org}$ baseline values sit at ∼−30.2‰ (Vienna Peedee belemnite [VPDB]) and begin climbing to ∼−29.5‰ in the latest Katian Stage. Values are steady between −29.5‰ and −29.0‰ in the lower half of the Hirnantian Stage and then peak at ∼−28.5‰ before decreasing in the uppermost Hirnantian beds. By the first appearance of

Akidograptus ascensus, marking the base of the Silurian System, the δ¹³C$_{org}$ values have returned to the pre-excursion baseline (Fig. 3).

The GSSP for the base of the Silurian System is at Dob's Linn, Scotland (Holland, 1985), where the first appearance of the graptolite *A. ascensus* provides the biostratigraphic tie

Figure 2. (A) Stratigraphy and biostratigraphy of the Ellis Bay Formation and adjoining beds, modified from Melchin (2008). Position of the Katian-Hirnantian boundary is contentious; most biostratigraphers argue for the base of the entire Ellis Bay Formation, and chemostratigraphers argue for the base of the Laframboise Member. See Figure 7 for lithological legend. (B) Generalized stratigraphy of Anticosti Island, modified from Petryk (1981); Long and Copper (1987a); Long (2007). H.—Hirnantian.
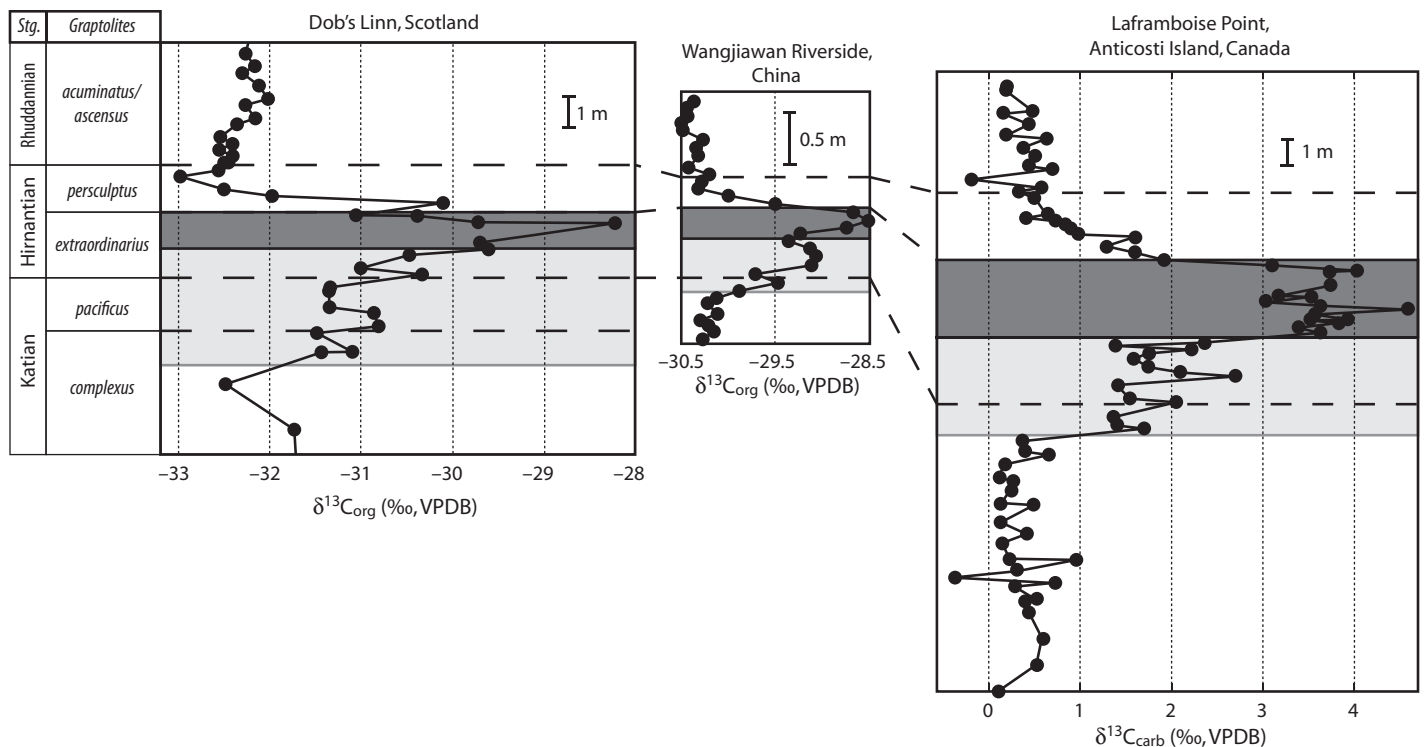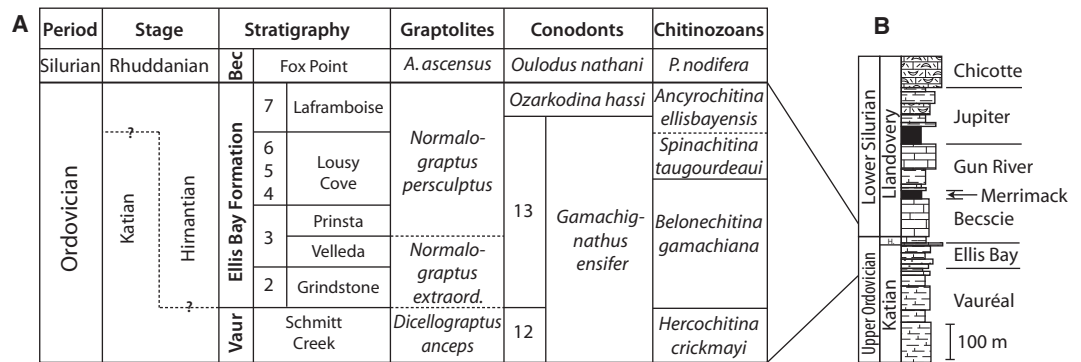
Figure 3. Carbon isotope records and graptolite biozonation from Dob's Linn, Scotland (Silurian global stratotype section and point [GSSP]; Underwood et al., 1997), Wangjiawan Riverside (180 m from Hirnantian GSSP; Chen et al., 2006), and Laframboise Point, Anticosti Island (current study). Locations of graptolite zones (dashed lines) are documented for Dob's Linn and Wangjiawan, but are inferred here for Anticosti, based on matching distinctive patterns in the δ¹³C record. The light shading identifies the first phase of the isotope excursion (initial rise); the dark shading represents the second phase (maximum values attained). The inferred correlation of Anticosti Island stratigraphy with the GSSPs is based on the high-resolution carbon isotope stratigraphy presented here. VPDB—Vienna Peedee belemnite.

point (Melchin and Williams, 2000). The GSSP is dominated by graptolitic shales, and Underwood et al. (1997) documented an ~+3‰ excursion in $\delta^{13}C_{org}$ coincident with the Hirnantian Stage (Fig. 3). Pre-excursion $\delta^{13}C_{org}$ values are ~−32‰. Values in the latest Rawtheyan (end Katian Stage) climb to ~−30.5‰. The Hirnantian beds peak at ~−28.5‰ before decreasing. The basal Silurian beds begin at the pre-excursion baseline of ~−32‰.

The positive $\delta^{13}C_{org}$ excursions at Dob's Linn and Wangjiawan Riverside both begin in the latest Katian Stage, and they are both completely finished by the base of the Silurian System. Furthermore, both excursions are characterized by a rise to an initial elevated plateau, and then a sharper spike to maximum values, followed by a quick decline to pre-excursion baseline (Fig. 3). Thus, the Hirnantian Stage at both GSSPs is characterized by enriched $\delta^{13}C_{org}$ values, with no intervening return to baseline.

The Hirnantian positive carbon isotope excursion has been identified in Laurentia (Orth et al., 1986; Long, 1993; Finney et al., 1999; Kump et al., 1999; Bergström et al., 2006; Melchin and Holmden, 2006; LaPorte et al., 2009; Young et al., 2010), South China (Wang et al., 1993, 1997; Chen et al., 2006; Fan et al., 2009; Yan et al., 2009; Zhang et al., 2009), and Baltica (Kaljo et al., 2001, 2004, 2008; Brenchley et al., 2003; Young et al., 2010). Most of these reports have focused on either $\delta^{13}C_{carb}$ or $\delta^{13}C_{org}$, but not both, and few studies that have examined both proxies report reproducible excursions in both phases. Because of the glacioeustatic sea-level fall associated with contemporaneous Gondwanan glaciation, Hirnantian strata are not well represented in the shallow-marine sedimentary record, and many Hirnantian sections probably contain hiatuses (Brenchley et al., 2003; Bergström et al., 2006). This fact has contributed to debate over the shape and magnitude of the carbon isotope excursion. Despite intra- and interbasinal variability, reproducible Hirnantian $\delta^{13}C$ excursions have been identified on all three paleocontinents.

MATERIALS AND METHODS

### Field Work and Sample Preparation

We logged and sampled 16 sections through the Ellis Bay and lower Becscie Formations during the summers of 2008 and 2009 (Fig. 1). We focused our high-resolution studies on the Laframboise Member of the Ellis Bay Formation, where previous workers (Orth et al., 1986; Long, 1993; Brenchley et al., 1994; Desrochers et al., 2010; Young et al., 2010) had identified the Hirnantian $\delta^{13}C_{carb}$ excursion. The strati-

raphy of the western end of the island is represented by a composite section assembled from coastal outcrops measured from English Head to Laframboise Point and Cape Henri (Fig. 4). The strata of the east-central portion of the island are represented by outcrops along the bluffs flanking the Salmon River (9 Mile Pool and 8 Mile Pool), and by sections exposed in stream cuts and by the road at Macaire Creek and a tributary of the Natiscotec River (Fig. 5). The eastern portion of the island is represented by a composite section assembled from coastal outcrops between Lousy Cove and Fox Point (Fig. 6). Coordinates of each section are listed in Table 1.

In the course of stratigraphic logging, we collected and cataloged fresh fist-sized hand samples at regular stratigraphic intervals. Samples were subsequently slabbed with a rock saw. Material for $\delta^{13}C_{carb}$ and $\delta^{18}O_{carb}$ analyses was obtained by drilling out ~100 mg of carbonate powder from each slab with a dental drill, targeting fine-grained mudstone where possible. An additional slab from each sample was crushed to a homogeneous powder in a Spex 8515 shatterbox with an aluminum carbide vessel. Approximately 1 g of this powder was reacted with an excess of 6 N HCl to remove carbonate minerals in preparation for $\delta^{13}C_{org}$ analysis. The

acid-insoluble residue was rinsed three times in deionized water, dried in a 70 °C oven overnight, homogenized with a mortar and pestle, and weighed. Aliquots of the insoluble residue were used for the $\delta^{13}C_{org}$ analyses.

Mass Spectrometry

Carbonate carbon isotope ratios were measured at both Washington University and Harvard University. At Washington University, ~100 µg samples of drilled carbonate powder were reacted for 4 h at 72 °C with an excess of 100% H_3PO_4 in He-flushed, sealed tubes. Evolved CO_2 was sampled with a Finnigan Gas Bench II, and isotopic ratios were measured with a Finnigan MAT 252 or Delta V Plus. Isotopic measurements were calibrated against NBS-19, NBS-20, and two in-house standards, with analytical errors of <0.1‰ (1σ) for $\delta^{13}C_{carb}$ and <0.2‰ (1σ) for $\delta^{18}O_{carb}$. At Harvard University, a VG Optima dual inlet mass spectrometer with a modified Isocarb preparation device was used. Approximately 1 mg of each sample was reacted in a 90 °C common H_3PO_4 bath for 8–10 min. Liberated CO_2 gas was collected and purified cryogenically. Sample gas and an in-house reference gas were analyzed four times each in the
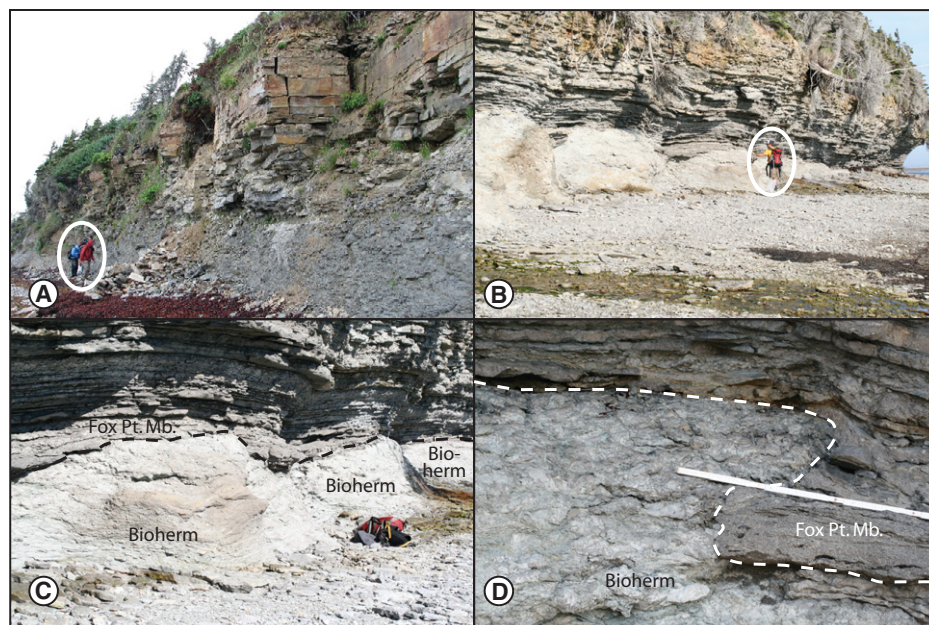
Figure 4. Photomontage of outcrops used in composite section of the Ellis Bay Formation at Laframboise Point, western sector of Anticosti Island. (A) Hummocky cross-stratified fine carbonate grainstones overlie nodular lime mudstones at Laframboise Point (sections D804 and 901). (B) Bioherms of the Laframboise Member are overlain by Becscie Formation skeletal grainstones (D804 and 901). (C–D) Details of contact between Laframboise Member and Becscie Formation at Laframboise Point demonstrating the complex relationship between the Laframboise bioherms and the overlying Becscie skeletal grainstones. Backpack for scale in C. Visible portion of measuring stick in D is 65 cm long.
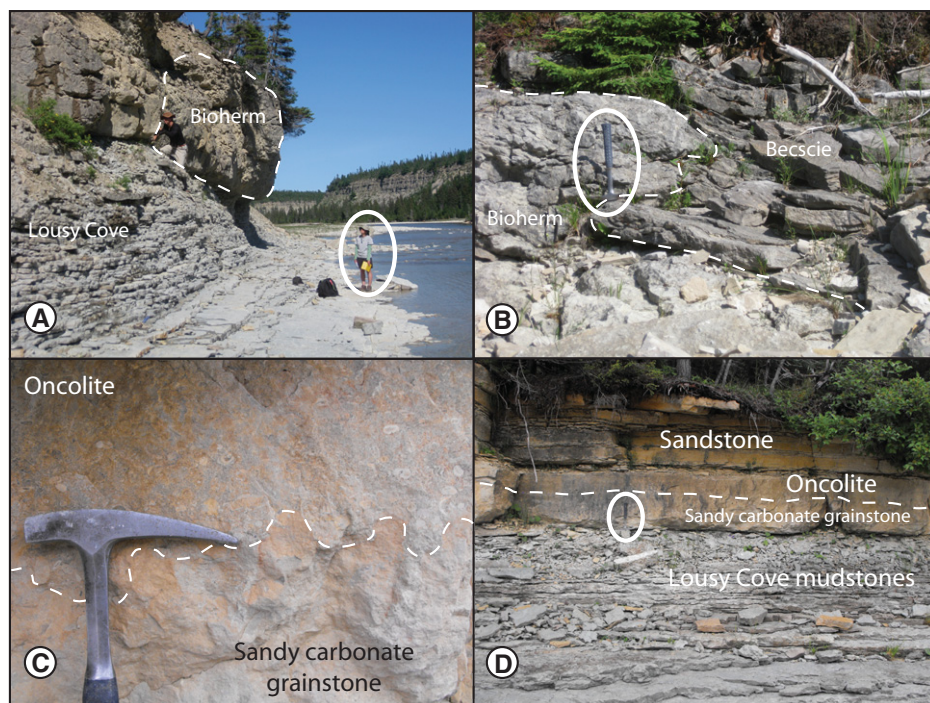
Figure 5. Photomontage of outcrops from the east-central sector at Salmon River and Macaire Creek. (A) Bioherms of the Laframboise Member overlying Lousy Cove Member (left bank of Salmon River). (B) Contact between Laframboise bioherms and Becscie skeletal grainstones (right bank of Salmon River). (C) Detail of Laframboise Member, illustrating transition from massive sandy carbonate grainstone to oncolite platform bed, which occurs at the level of the head of the pick (section D816). (D) Contact between Lousy Cove and Laframboise Members, 100 m upstream from section D816; bioherms are not developed here.

course of each measurement. The CM-2 Cararra Marble standard was measured seven times during each run of 53 samples to calibrate samples to the VPDB standard, provide a measure of uncertainty, and monitor potential memory effect associated with the common acid bath system. Analytical uncertainties (1σ) for both $\delta^{13}C_{carb}$ and $\delta^{18}O_{carb}$ were <0.1‰, and memory effect (the contribution of any CO_2 gas from the previous sample due to use of a common acid bath) for $\delta^{13}C_{carb}$ was consistently <0.2‰, as determined by measurement of within-run standards. A subset of samples was measured at both laboratories as a check of interlaboratory consistency, and no discernible difference was observed between them.

Organic carbon isotopes were measured by combusting tin cups containing acid-insoluble residue in a Costech ECS 4010 Elemental Analyzer at 1000 °C. The mass of insoluble residue combusted was varied for each sample to give a constant peak size for CO_2 on the mass spectrometer. Evolved gas flowed through an oxidation/reduction furnace before entering a Finnegan Delta V Plus for isotopic analysis. Isotopic measurements were calibrated against NBS-21 graphite, IAEA-C6 sucrose, and in-house acetanilide standards. All samples were measured in duplicate with a reproducibility of <0.2‰ (1σ) and are reported relative to the VPDB scale.

STRATIGRAPHY AND FACIES

The stratigraphy and biostratigraphy of the Ellis Bay and Becscie Formations have been the subject of numerous careful and detailed studies (e.g., Lake, 1981; McCracken and Barnes, 1981; Petryk, 1981; Nowlan, 1982; Long and Copper, 1987a, 1987b; Barnes, 1988; Sami and Desrochers, 1992; Farley and Desrochers, 2007; Desrochers et al., 2010; Achab et al., 2010). In this section, we provide a brief outline of our stratigraphic observations in order to provide the context for our chemostratigraphic data.

The stratigraphic expression of the Ellis Bay and Becscie Formations varies along the length of the outcrop belt. Facies vary laterally from west to east, especially in the Ellis Bay Formation; in the west, limestones dominate with minor shales, whereas more sandy facies occur in the east (Petryk, 1981; Long and Copper,

1987a). The western sector (coastal outcrops at the western tip of the island and around Laframboise Point) constitutes one distinct set of facies, dominated by carbonate rocks with very little siliciclastic input (Fig. 4). The east-central sector (outcrops at Natiscotec River tributary, Salmon River, and Macaire Creek) constitutes a second distinct suite of facies; here, the Laframboise Member is thinner than in the west, and siliciclastic sands are present in the lowermost Fox Point Member (Fig. 5). The eastern sector (coastal outcrops from Lousy Cove to Fox Point) constitutes the third distinct suite of facies (Fig. 6). Here, the siliciclastic content is at a maximum, and the Laframboise Member has reduced thickness. The Laframboise Member is not well exposed in outcrop in a significant portion of the island's center. This leads to an uneven distribution of studied outcrops in our transect across the basin (Fig. 1). Locations and names of sections are given in Table 1.

Observation at outcrop and microscopic scales reveals excellent preservation of sedimentary structures and textures. There has been minimal recrystallization of carbonate matrix or skeletal material. Evidence of dolomitization is rare. Skeletal grains are often abundant and well preserved (GSA Data Repository Fig. DR1A and DR1D[1]). Bioturbation textures occur in many facies, and burrows are preserved in fine detail (Fig. DR1B and DR1C [see footnote 1]). Oncolites preserve internal laminations (Fig. DR1E [see footnote 1]).
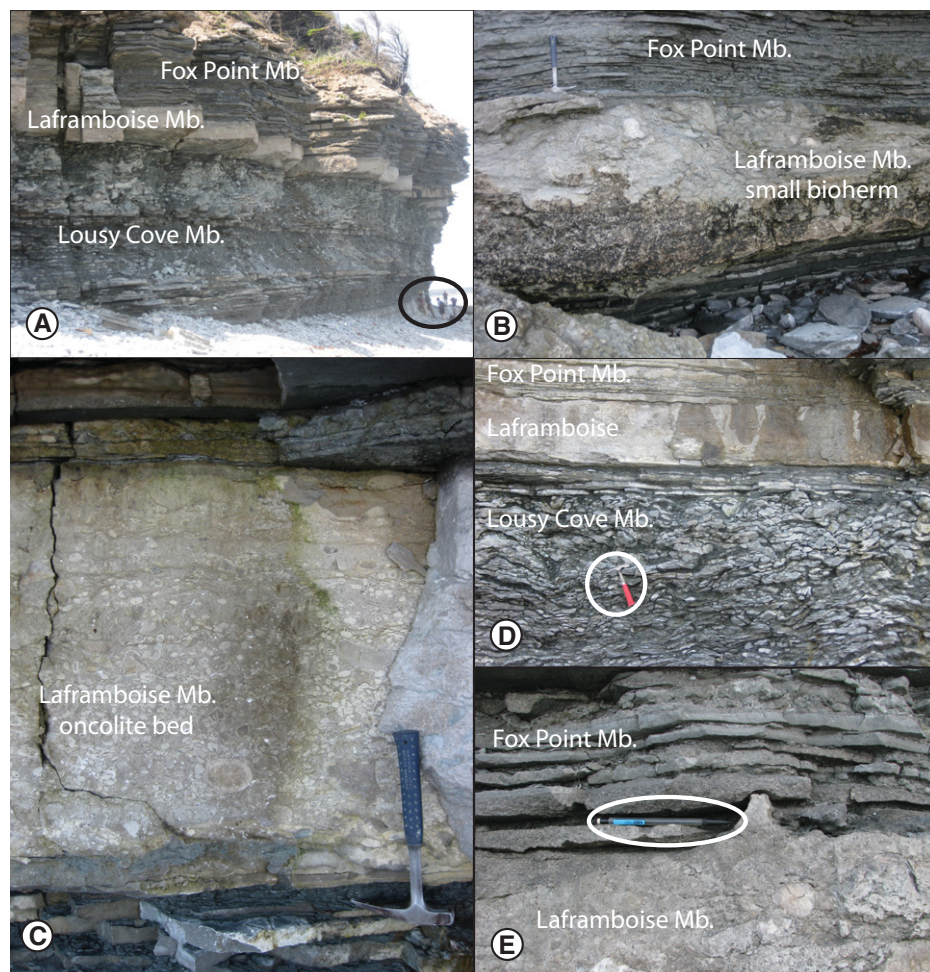
Lousy Cove Member (Ellis Bay Formation)

In the western sector at section D804 and 901 (Laframboise Point), exposure of the Lousy Cove Member begins with recessive greenish-gray lime mudstones with a nodular texture and rare centimeter-scale grainstone beds. This facies is sharply overlain by a gray calcisiltite unit with 10–40-cm-thick beds and discontinuous mud stringers. The calcisiltite becomes more massive and platy up-section and develops hummocky cross-stratification with submeter wavelength in the uppermost 2 m of the member (Fig. 4A). The upper surface of the Lousy Cove Member is a blackened, scoured surface with ~5 cm of erosional relief.

In the east-central sector at sections D814–D816 (Salmon River upstream, 9 Mile Pool) and 909 (Salmon River downstream, 8 Mile Pool), the Lousy Cove Member begins with greenish-gray lime mudstone with occasional

Figure 6. Photomontage of outcrops used in composite section of the Ellis Bay Formation between Lousy Cove and Fox Point, eastern Anticosti Island (section 914). (A) Laramboise Member (lightest strata) exposed on the east coast. (B) Detail of biohermal texture in Laramboise Member. (C) Detail of oncolitic texture within Laramboise Member. (D) Massive Laramboise Member between disturbed beds of upper Lousy Cove Member (below) and well-bedded grainstones of Becscie Formation (above). (E) Erosional contact between overlying Becscie Formation skeletal grainstones and underlying oncolite platform bed of Laramboise Member.

silt and hummocky cross-stratification. This unit is overlain by several meters of rubbly weathering concretionary silty limestone. Two meters of mudstone separate the concretionary layer from a 4-m-thick unit composed of very dark-gray planar laminated limestone with *Chondrites*, interbedded with gray brachiopod-bearing lime mudstone. Near the top, the member is composed of thin calcareous shales interbedded with both planar and cross-stratified sandy grainstone beds (Figs. 5A and 5D). The uppermost unit is a 50-cm-thick, massive buff-colored sandy carbonate grainstone with a pitted and scoured top surface (Fig. 5C). At section 912 at Macaire Creek, mudstone rip-up clasts are found in the massive sandy grainstone.

In the east sector at section 914 (Lousy Cove, Fig. 6A), the bottom exposure of the Lousy Cove Member is a cross-bedded calcarenite bed with 10–20-cm-thick foreset beds. Intraclasts are pervasive, and the top of the unit is burrowed, with a well-rounded quartz pebble lag. This is succeeded by a bioturbated nodular muddy wackestone with corals and brachiopods. Three meters of shales interbedded with calcareous mudstones and carbonate grainstones lie above the nodular layer. There are frequent skeletal (often crinoid) packstone and grainstone interbeds, some of which form gutters. Twenty centimeters of lime grainstones with hummocky cross-stratification separate the shales from a 1-m-thick zone of intense internal deformation

(Fig. 6D). This disturbed zone is composed of shales interbedded with siltstones and calcareous mudstones. Above the convoluted unit, there are 20 cm of undisturbed beds of the same lithology. These are capped by a light-colored resistant grainstone full of rip-up clasts of the underlying bed. The top of this bed, which is the top of the Lousy Cove Member, is clearly an erosional surface, with upright aulecerid stromatoporoid fossils truncated by the base of the overlying Laramboise Member oncolite.

**Laramboise Member
(Ellis Bay Formation)**

The Laramboise Member is defined to include the oncolite platform bed (Petryk, 1981), the large distinctive bioherms, and interbiohermal limestones (Long and Copper, 1987a; Copper, 2001). In the west sector (sections D804 and 901 at Laramboise Point), the oncolite bed is 10–20 cm thick and fills pits and scours in the underlying Lousy Cove strata. The biohermal unit sits on top of the oncolite bed and consists of meter-scale isolated bioherms and interbiohermal limestone (Figs. 4B, 4C, and 4D). The bioherms host a complex biota; to first order, they contain abundant calcimicrobial textures with tabulate and rugose corals. Interbiohermal beds of the Laramboise Member are largely lime mudstone and wackestone.

The contact with the overlying Fox Point Member of the Becscie Formation is complex. Interbiohermal beds in the 50 cm below the level of the bioherm tops include skeletal grainstones composed of brachiopod, trilobite, coral, bryozoan, and echinoderm material, assigned to the Fox Point Member of the Becscie Formation. In some places, these grainstones appear to truncate the bioherms, but in other places, the bioherms can be seen to be growing out over discontinuous grainstone beds (Fig. 4D); this complicated interfingering geometry suggests that the Laramboise Member bioherms were still growing, perhaps sluggishly, when the first incursion of Becscie skeletal grainstones was deposited.

In the east-central sector, the oncolite platform bed of the Laramboise Member is 30–40 cm thick and contains abundant oncoids, corals, and stromatoporoids (Fig. 5C). It has an erosional contact with the underlying massive sandy grainstone unit at the top of the Lousy Cove Member. The oncolite bed grades into overlying bioherms where they are present. The bioherms are not as closely spaced in the east-central sector compared as to the west, and some reach thicknesses of 8 m. In exposures where bioherms are absent, the oncolite bed constitutes the entirety of the Laramboise Member (Figs. 5C and 5D).

TABLE 1. LOCATIONS OF MEASURED SECTIONS USED IN THE STUDY

Anticosti Island Section Locations

Section ID	Latitude (°N)	Longitude (°W)	Location name
Western sector			
D821	49°54.072′	64°29.458′	English Head
D801	49°49.567′	64°26.574′	Junction Cliff
D802	49°48.855′	64°25.781′	
D803	49°48.646′	64°25.520′	
D804, 901	49°48.350′	64°25.259′	Laframboise Point
D805	49°47.763′	64°22.735′	Cape Henry
D806	49°47.545′	64°23.066′	Cape Henry
East-central sector			
920	49°29.530′	62°32.631′	Natiscotec tributary
911	49°23.853′	62°23.583′	9 Mile Pool, right bank
D816, D817, 908	49°24.015′	62°23.175′	9 Mile Pool, left bank
D814, 909A/B	49°24.328′	62°21.420′	8 Mile Pool
912, 912A	49°22.762′	62°12.320′	Macaire Creek Quarry
D813	49°22.838′	62°12.230′	Macaire Creek stream A
D815	49°22.498′	62°12.225′	Macaire Creek stream B
Eastern sector			
914/A/B	49°19.198′	61°51.399′	Lousy Cove

CHEMOSTRATIGRAPHIC RESULTS

Stable isotopic data are tabulated in GSA Data Repository Table DR1 (see footnote 1).

Western Anticosti Island

At Laframboise Point in the west (Fig. 7), Lousy Cove Member mudstones record a baseline $\delta^{13}C_{carb}$ value of ~0.5‰. An isotopic discontinuity separates the top of the Lousy Cove mudstones from the overlying sandy carbonate grainstones. In the coarser unit, $\delta^{13}C_{carb}$ and $\delta^{13}C_{org}$ rise by 2‰. Although there is strong field evidence for an erosional surface separating the grainstones from the oncolite platform bed, the continuity of $\delta^{13}C_{carb}$ across this surface indicates that not much time is missing at this boundary. Above the oncolites, $\delta^{13}C_{carb}$ climbs to +4‰ and fluctuates around that value through the biohermal unit. Similarly, $\delta^{13}C_{org}$ shows a parallel rise below the oncolite bed and fluctuations around the maximum above it (Fig. 7). Up section, high-resolution sampling shows that there is a smooth decline in $\delta^{13}C_{carb}$ from the +4‰ maximum down to +0.5‰ from the top of the biohermal unit

In the east sector at section 914 (Lousy Cove), the oncolite platform bed of the Laframboise Member is 50–60 cm thick and contains abundant corals and oncolites (Fig. 6A). The base truncates aulecerid stromatoporoid fossils of the underlying Lousy Cove Member. Oncolites are nucleated around clasts of the underlying bed (Fig. 6C). Bioherms are less abundant here than in the other sectors, and they are considerably smaller (Fig. 6B).

Fox Point Member (Becscie Formation)

The base of the Becscie Formation at sections D804 and 901 (Laframboise Point) in the western sector is characterized by 1 m of interbedded grainstones and lime mudstones (Figs. 4B, 4C, and 4D) that appear in some places to interfinger with the Laframboise Member bioherms (Fig. 4D). Some grainstones display hummocky cross-stratification or wave ripples. A few meters up-section, the grainstone beds become thinner and less common, and mudstone dominates.

In the east-central sector, the Becscie Formation begins with thin resistant sandstone that overlies the Laframboise oncolite platform bed where bioherms are absent (Fig. 5D). The sandstone frequently displays low-angle cross-stratification. Above the sandstone, the Fox Point Member typically becomes recessive and poorly exposed for 2 to 4 m. At section 911, on the right bank of the Salmon River, across from the upstream section (9 Mile Pool), bioherms of the Laframboise Member are directly overlain with skeletal grainstones with a diverse fauna, including ramose bryozoans and nautiloids.

The base of the Fox Point Member at section 914 (Lousy Cove) in the eastern sector displays

5 to 10 cm of relief on the underlying Laframboise Member (Fig. 6E). Dark-gray skeletal grainstones at the bottom of the member are replaced with hummocky cross-stratified fine calcarenite within 2 m of the base. Normally graded bioclastic interbeds are common.
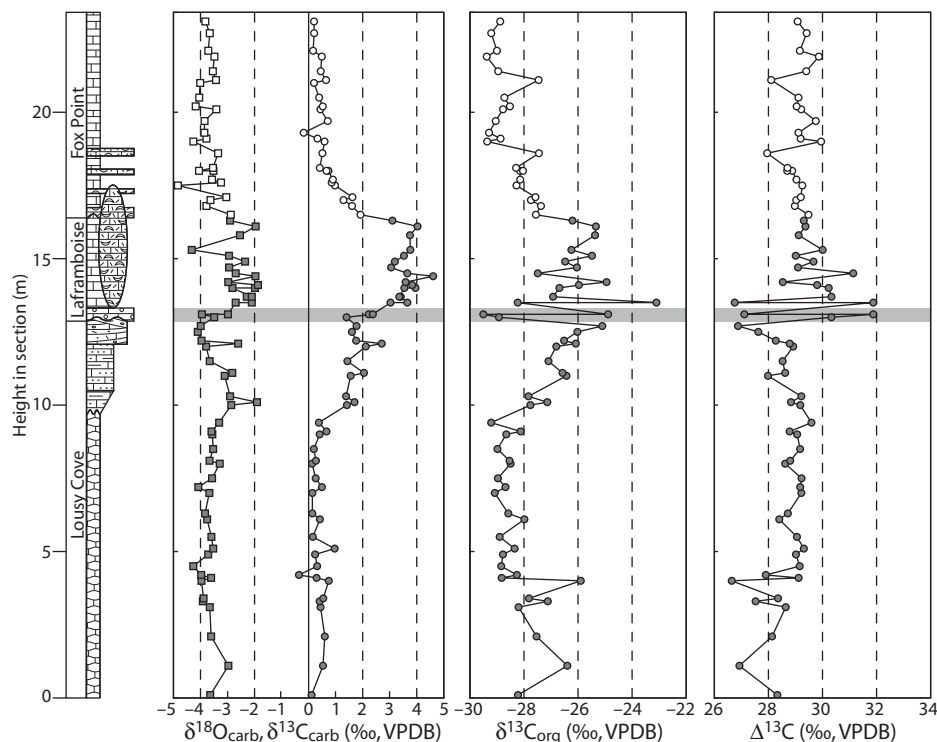

Figure 7. Geochemistry and lithostratigraphy of sections D804 and 901 from Laframboise Point, western Anticosti Island. Oncolite platform bed data are shaded in gray. Filled data points are from Ellis Bay Formation; open data points are from Becscie Formation. See Figure 8 for legend. VPDB—Vienna Peedee belemnite.

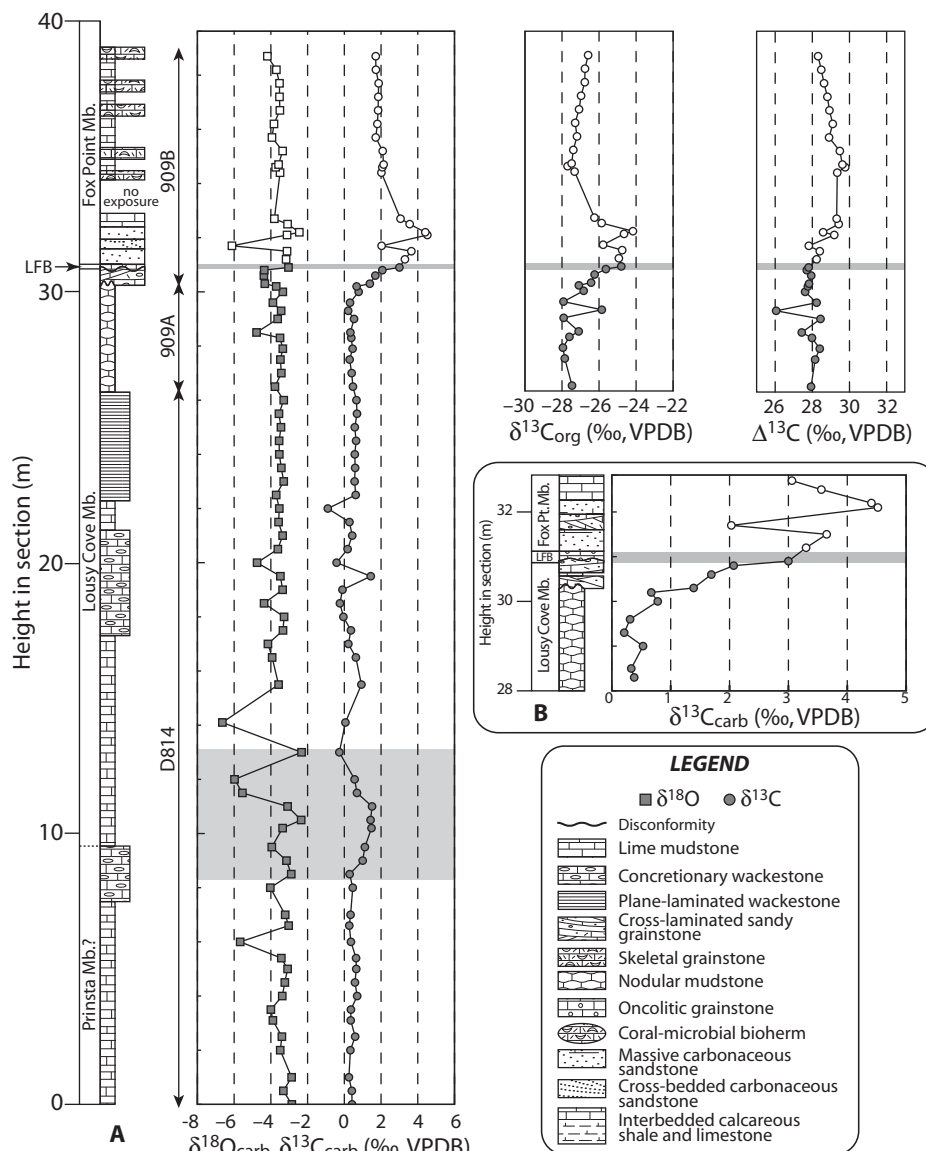through the lowest 2 m of the Becscie skeletal grainstones. The $\delta^{13}C_{org}$ values are observed to decline in parallel.

East-Central Anticosti Island at Salmon River and Macaire Creek

At Salmon River, in the east-central sector of the island, the Laframboise Member is exposed on the riverbanks for over a kilometer. At the downstream section (8 Mile Pool, section 909, Fig. 8), the member is <1 m thick and lacks bioherms. The $\delta^{13}C_{carb}$ pattern in the underlying Lousy Cove Member has a well-defined baseline of +0.5‰. Both $\delta^{13}C_{carb}$ and $\delta^{13}C_{org}$ begin to climb 2 m below the Lousy Cove–Laframboise contact. There is a ~1‰ step up in both proxies across the base of the oncolite platform bed, above which $\delta^{13}C_{carb}$ continues to rise to +4‰. The cross-stratified sandstone bed at the base of the Fox Point Member hosts a 2‰ downturn in $\delta^{13}C_{carb}$ (and a simultaneous drop in $\delta^{18}O_{carb}$), which may be a diagenetic artifact due to high cement content of the bed. Above the cross-stratified bed, $\delta^{13}C_{carb}$ rises again to a peak of +4.5‰, before declining to +3‰ at the top of the exposure. In this interval, $\delta^{13}C_{org}$ moves in the same direction as $\delta^{13}C_{carb}$, but $\Delta^{13}C$ (= $\delta^{13}C_{carb}$ − $\delta^{13}C_{org}$) steps up to ~29‰. The succeeding 2 m of stratigraphy are not exposed. Five meters of the Fox Point Member are exposed at the top of the outcrop, and this interval shows $\delta^{13}C_{carb}$ values constant at +1.8‰, i.e., significantly enriched relative to the pre-excursion values in the Lousy Cove Member. It is also enriched relative to the lithologically equivalent strata at Laframboise Point at the western end of Anticosti Island. Throughout the $\delta^{13}C_{carb}$-enriched beds, $\delta^{13}C_{org}$ values monotonically increase such that $\Delta^{13}C$ returns to its pre-excursion value of 28‰ at the top of the section.

Below the Laframboise Member, at the downstream locality (8 Mile Pool, section D814, Fig. 8), $\delta^{13}C_{carb}$ values are relatively invariant at ~0‰, with one significant exception; a positive excursion to +1.5‰ occurs at a lithological change ~20 m below the Laframboise Member that may correspond to the Prinsta–Lousy Cove boundary. Approximately 15 m of Lousy Cove stratigraphy with an isotopic composition close to 0‰ separate this excursion from the larger $\delta^{13}C_{carb}$ excursion described previously (Fig. 8).

Two kilometers upstream (9 Mile Pool, sections D816, 908, and 911; Fig. 9), bioherms are variably present in the Laframboise Member (Fig. 5). In the mudstones of the upper Lousy Cove Member, $\delta^{13}C_{carb}$ maintains a baseline value of 0.7‰. Isotope values in the uppermost Lousy Cove grainstones in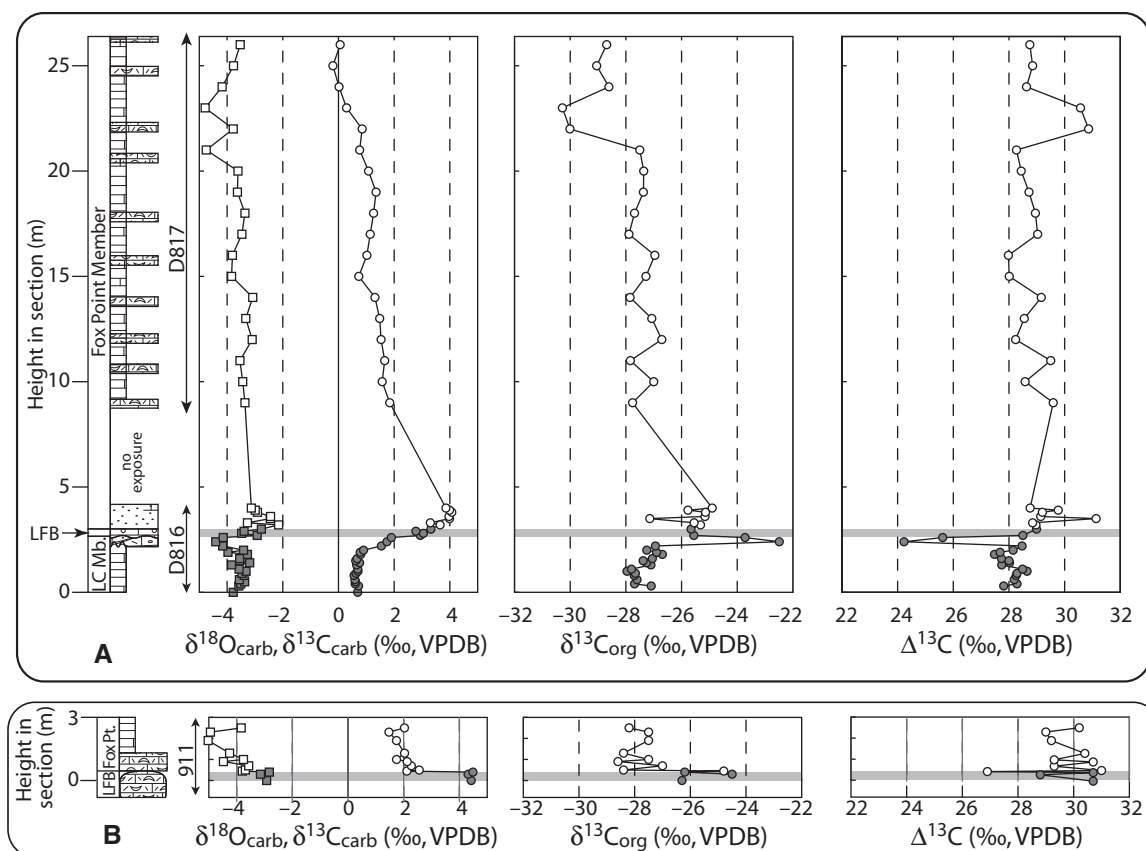crease to +2‰, and in the overlying Fox Point Member carbonaceous sandstones, $\delta^{13}C_{carb}$ reaches a peak of +4.1‰ (Fig. 9A). There are two $\delta^{13}C_{carb}$ discontinuities: one across the surface separating the Lousy Cove mudstones from the Lousy Cove sandy grainstones, and another across the Lousy Cove–Laframboise contact. Measurements from the top of a Laframboise bioherm into the overlying skeletal grainstones of the Becscie Formation (section 911; Fig. 9B) show that the uppermost biohermal carbonates have $\delta^{13}C_{carb}$ of ~+4.5‰. A step-function drop to just under +2‰ in the lowermost Becscie Formation follows these enriched values. The Becscie Formation remains isotopically enriched over the next 10 m of stratigraphy, declining over that interval until it reaches 0‰ at 20 m above the top of the Laframboise Member.

Ten kilometers east of Salmon River at Macaire Creek (sections D815 and 912; Fig. 10), $\delta^{13}C_{carb}$ values jump discontinuously across the surface separating the Lousy Cove mudstones from the overlying Lousy Cove sandy

Figure 8. (A) Geochemistry and lithostratigraphy of the composite section from the Salmon River downstream section, central Anticosti Island. Data are from sections D814 and 909A/B. (B) Detailed stratigraphic column of section 909A/B at the Ellis Bay–Becscie Formation contact. Thin oncolite platform bed data are shaded in gray. Pre-Hirnantian $\delta^{13}C_{carb}$ excursion is shaded in gray at the Prinsta–Lousy Cove boundary. Filled data points are from Ellis Bay Formation; open data points are from Becscie Formation. LFB—Laframboise Member. VPDB—Vienna Peedee belemnite.

Figure 9. (A) Geochemistry and lithostratigraphy of the composite section from the left bank of the Salmon River upstream section, central Anticosti Island. Data are from sections D816 and D817. Section D816 was measured between bioherms. (B) Geochemistry and lithostratigraphy of the section from the right bank of the Salmon River upstream section, central Anticosti Island. Data are from section 911, through uppermost exposure of partially exposed bioherm and overlying Becscie strata. Oncolite platform bed data are shaded in gray. Filled data points are from Ellis Bay Formation; open data points are from Becscie Formation. LC—Lousy Cove, LFB—Laframboise Member, VPDB—Vienna Peedee belemnite. See Figure 8 for legend.

grainstones. Isotope values within the sandstone rise from 2‰ to 4‰ and then decline toward 2‰. The lower Becscie Formation local minimum observed within the cross-stratified grainstones at Salmon River (Fig. 8) is not reproduced at Macaire Creek. Organic carbon isotope values decline above the oncolite bed, in parallel with $\delta^{13}C_{carb}$; however, they do so at a different rate, producing rising $\Delta^{13}C$ values. The lower Becscie Formation is poorly exposed above the sandstone at this outcrop, but the few measured samples in the lowermost 2 m register $\delta^{13}C_{carb}$ of ~+2‰, i.e., significantly elevated from pre-excursion baseline.

Eastern Anticosti Island

The Laframboise Member is <1 m thick at exposures on the east coast of the island (Fig. 6). It is largely oncolitic from the base to the top. There is a large (>3‰) discontinuity in $\delta^{13}C_{carb}$ across the lower contact with the Lousy Cove mudstones (Fig. 11). The transition to the Fox Point Member of the Becscie Formation does not include an immediate return to baseline $\delta^{13}C_{carb}$ values. The lowest 4 m of the Becscie Formation on the east coast are enriched by 2‰ relative to the west.

## DO ANTICOSTI ISLAND STABLE ISOTOPE RECORDS REFLECT A PRIMARY SEAWATER SIGNAL?

Diagenetic Considerations

The carbonate rocks exposed on Anticosti Island are preserved exceptionally well. An analysis of the conodont color alteration index (CAI) of specimens from the Ellis Bay and Becscie Formations shows that most conodont elements have a CAI of 1.0–1.5, corresponding to maximum burial temperatures of less than 90 °C (McCracken and Barnes, 1981). The structure of the basin is simple. Strata across the island have a constant dip of ~2° to the southwest (Fig. 1), and few faults are exposed, indicating that the rocks of the island have experienced minimal deformation. Microscopic analysis of polished slabs (Fig. DR1 [see footnote 1]) and thin sections confirms observations made at the outcrop scale, i.e., that there has been little observable recrystallization. The relatively pristine state of the Anticosti carbonate rocks indicates that they have not been subject to extensive diagenetic alteration.

Carbonate rocks that have been isotopically altered by meteoric diagenesis are frequently depleted in $\delta^{18}O_{carb}$ because meteoric waters tend to have very low oxygen isotope ratios. Because diagenetic fluids contain little carbon but abundant oxygen, carbonate rocks that have experienced extensive diagenetic overprinting can maintain original carbon isotope

Figure 10. Geochemistry and lithostratigraphy of the composite section from the Macaire Creek section, central Anticosti Island. Data are from sections D815 and 912. Oncolite platform bed data are shaded in gray. Filled data points are from Ellis Bay Formation; open data points are from Becscie Formation. LFB—Laframboise Member, VPDB—Vienna Peedee belemnite. See Figure 8 for legend.
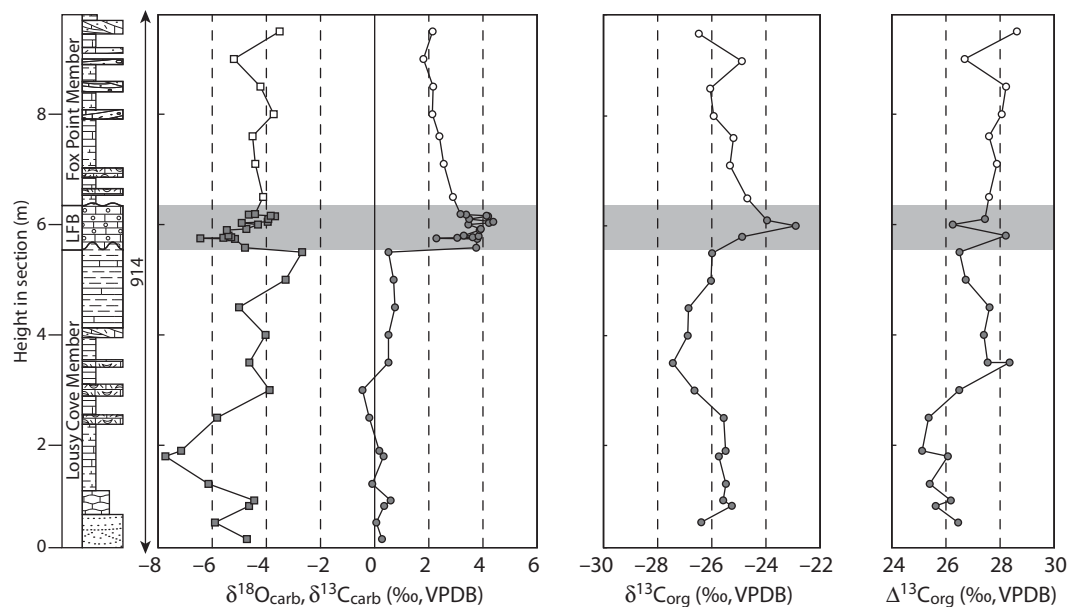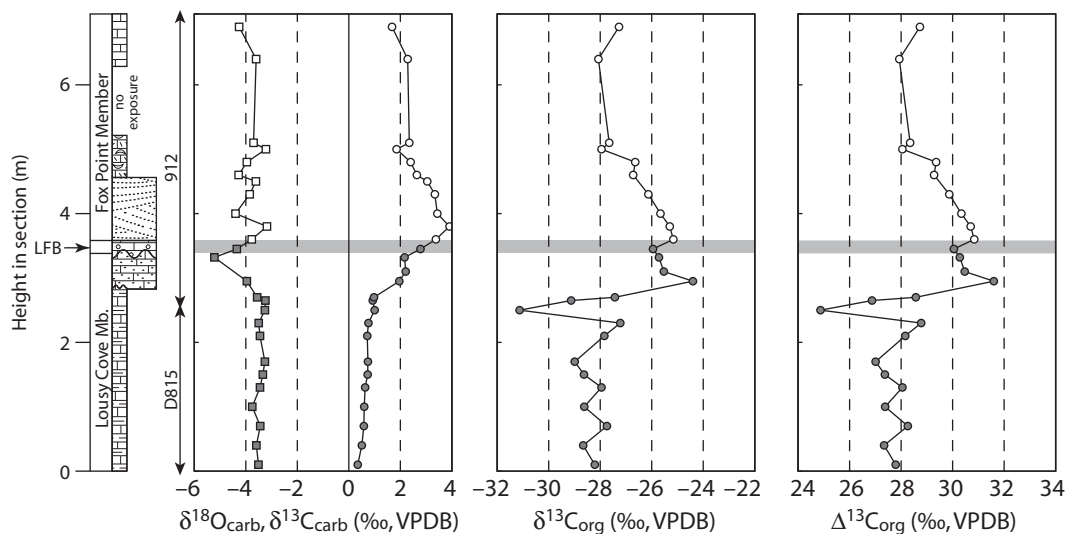
Figure 11. Geochemistry and lithostratigraphy of the composite section from Lousy Cove to Fox Point Members, eastern Anticosti Island. Data are from section 914. Oncolite platform bed data are shaded in gray. Filled data points are from Ellis Bay Formation; open data points are from Becscie Formation. LFB—Laframboise Member, VPDB—Vienna Peedee belemnite. See Figure 8 for legend.

ratios despite exhibiting very depleted oxygen isotope ratios (Banner and Hanson, 1990). However, any small amount of alteration of $\delta^{13}C$ during meteoric diagenesis would likely be derived through reaction with respired carbon from decomposed organic matter. This respired carbon would have a highly depleted $\delta^{13}C$ composition, thus depleting the $\delta^{13}C_{carb}$ signature of the meteorically altered carbonate rocks. We can test the Anticosti Island samples for this diagenetic effect by examining the rocks deposited in the shallowest water depths, which would therefore be the rocks most readily exposed to meteoric diagenesis. As discussed already, the Laframboise Member represents the shallowest water depth

recorded in the Anticosti Basin, and cathodoluminescence studies have suggested some degree of meteoric alteration. However, examination of the isotopic record of this interval at Laframboise Point (the section for which the most data are available; Fig. 7) shows that Laframboise strata are enriched, not depleted, in both oxygen and carbon isotope ratios. This result rules out the possibility of meteoric alteration of the isotopic record.

The low conodont alteration index and lack of evidence for meteoric diagenesis suggest that $\delta^{13}C_{carb}$ values measured in Anticosti limestones likely reflect the $\delta^{13}C$ composition of the seawater from which they precipitated (Long, 1993; Desrochers et al., 2010; Young et al., 2010).

Lateral $\delta^{13}C$ Gradients in the Anticosti Basin?

Lateral gradients in $\delta^{13}C$ of up to 4‰ have been documented in modern seawater and sediment of Florida Bay and the Bahama Banks (Patterson and Walter, 1994), late Cenozoic sediments of the Bahamas (Swart and Eberli, 2005), and Paleozoic sedimentary rocks of the North American midcontinent (Holmden et al., 1998), all associated with carbonate platform and epeiric sea settings. These gradients can develop when platform waters are not efficiently mixed with the open ocean, allowing a geochemical evolution distinct from that of the open ocean. Depletion of $\delta^{13}C$ due to the oxidation of

isotopically light marine organic matter can occur during the "aging" of poorly mixed water on the platform top (Patterson and Walter, 1994).

In order to test whether a lateral $\delta^{13}C$ gradient existed in the Anticosti Basin, it is necessary to compare the $\delta^{13}C_{carb}$ values of coeval samples from across the basin. We perform this test first with strata hosting the positive carbon isotope excursion and second with older strata lower in the section.

The peak of the Laframboise Member $\delta^{13}C_{carb}$ excursion is of the same absolute value in all parts of the island; the maximum $\delta^{13}C_{carb}$ value measured in each of the three geographic sectors is 4.5‰. If a lateral gradient had existed, the expectation would be for maximum values of the excursion to vary as a function of distance from the shoreline (Immenhauser et al., 2003; Melchin and Holmden, 2006). The maximum value obtained in the western sector is 4.6‰ at section 901; the maximum value obtained in the east-central sector is 4.5‰ at section 911; the maximum value obtained in the east sector is 4.4‰ at section 914. The fact that this maximum value is invariant between each of the three geographic sectors of the basin is strong evidence that no basin-scale lateral carbon isotope gradient existed during the deposition of the Laframboise Member. Similarly, the baseline $\delta^{13}C_{carb}$ values of the pre-excursion Lousy Cove strata are consistent across the island, falling in a narrow range between 0.5‰ and 0.7‰, and exhibiting no systematic east-west variation. This suggests that no lateral carbon isotopic gradient existed in the time immediately before the start of the Hirnantian excursion.

For strata older than the top of the Lousy Cove Member, we appeal to previously published $\delta^{13}C_{carb}$ data tied to basinwide correlations of transgressive-regressive (TR) cycles of Desrochers et al. (2010) (Fig. DR2 [see footnote 1]). Desrochers et al. (2010) identified five TR cycles in the upper Vauréal and Ellis Bay Formations, which they traced across the length of the Anticosti Basin and interpreted as 400 k.y. eccentricity-forced Milankovitch cycles. Because these TR cycles are thought to be a response to glacioeustatic sea-level fluctuations, they should be isochronous. Therefore, boundaries between the TR cycles can serve as time lines, and the $\delta^{13}C_{carb}$ values at those boundaries can be compared in order to test for the existence of lateral isotopic gradients. The data are variable due to low sampling resolution and difficulties associated with precise selection of maximum regressive surfaces in conformable successions, but there is no systematic gradient to the $\delta^{13}C_{carb}$ values from one end of the island to the other (see supplementary information [see footnote 1]).

New and existing isotopic data for the Anticosti strata allow for basin-scale comparisons of $\delta^{13}C_{carb}$ gradients before and during the Hirnantian positive excursion. These $\delta^{13}C_{carb}$ data do not support the presence of a lateral isotopic gradient in the Anticosti Basin during the deposition of the Ellis Bay Formation.

$\delta^{18}O_{carb}$ as a Proxy for Climate Variables?

The potential for $\delta^{18}O_{carb}$ to provide detailed stratigraphic records of paleoclimate has long been recognized (Urey, 1947). Studies of the isotopic composition of foraminifera in Pleistocene deep-sea sediments elucidated the roles that temperature (Emiliani, 1966) and ice volume (Shackleton, 1967) have played in the $\delta^{18}O_{carb}$ record of marine carbonate sediments. In studies of Paleozoic carbonate rocks, significant advances have been made using the $\delta^{18}O_{carb}$ of low-Mg calcite shells, which are more resistant to diagenetic overprinting than other skeletal carbonate mineralogies (Veizer et al., 1999). In the present study, we focus not on brachiopod shell material, but on fine-grained micritic components that provide a stratigraphically continuous sampling opportunity. For this reason, we do not emphasize interpretations of the $\delta^{18}O_{carb}$ data. It should be noted that in the western sector, $\delta^{18}O_{carb}$ shows a positive excursion coincident with the $\delta^{13}C$ excursion in the Laframboise Member, as would be expected due to changes in temperature and $\delta^{18}O_{seawater}$ associated with glaciation (Fig. 7). However, this $\delta^{18}O_{carb}$ excursion is not reliably reproduced in the other measured sections.

COMPLETENESS AND STRATIGRAPHIC RANGE OF THE HIRNANTIAN POSITIVE ISOTOPE EXCURSION

Previous chemostratigraphic studies of the Hirnantian Stage on Anticosti Island and in the Baltics have concluded that Anticosti Island does not preserve the entirety of the Hirnantian positive carbon isotope excursion (e.g., Brenchley et al., 2003; Bergström et al., 2006). Comparing the original $\delta^{13}C$ data of Long (1993) with their data from Baltica, Brenchley et al. (2003) suggested that most of the $\delta^{13}C$ excursion was missing due to a significant stratigraphic gap within the Laframboise Member. Bergström et al. (2006) and Desrochers et al. (2010) reached a similar conclusion using enhanced data sets from Anticosti Island and argued that two hiatuses exist— one at the base of the oncolite platform bed, and one at the Ellis Bay–Becscie contact. As described in the following, our new chemostratigraphic data refine the timing and magnitudes

of the discontinuities and imply asynchronous deposition of the strata of the Laframboise and Fox Point Members across Anticosti Island (Fig. 12); the stratigraphic expression of the $\delta^{13}C$ excursion is different at the western end, the east-central sector, and the eastern end, as discussed next.

Base of the Hirnantian Stage on Anticosti Island

The stratigraphic extent of the Hirnantian Stage on Anticosti Island has been a contentious issue, with biostratigraphers often arguing that the entire Ellis Bay Formation is Hirnantian and chemostratigraphers arguing that only the uppermost Lousy Cove and Laframboise Members are Hirnantian. Copper (2001) and Jin and Copper (2008) considered the entire Ellis Bay Formation to be Hirnantian, based on their discovery of *Hindella* and *Eospirigerina* brachiopods at the bottom of the Grindstone Member and *Hirnantia* within the Prinsta Member. However, as reviewed in Kaljo et al. (2008), *Hindella* and *Eospirigerina* have their first appearances in Baltic sections in the Katian Stage and therefore may not be diagnostic of the Hirnantian Stage. Melchin (2008) recently identified graptolites indicative of the Hirnantian *Normalograptus persculptus* zone in the Lousy Cove Member. If these identifications are correct, (1) the base of the Hirnantian is below the Lousy Cove Member, and (2) the positive carbon isotope excursion in the Laframboise Member begins in the *N. persculptus* zone, and not in the *N. extraordinarius* zone (Melchin and Holmden, 2006; Melchin, 2008), as argued by Baltic chemostratigraphers (Brenchley et al., 2003; Kaljo et al., 2008). However, there has not been widespread agreement on the interpretation of the graptolite record (Delabroye and Vecoli, 2010).

Melchin (2008) suggested that a small $\delta^{13}C_{carb}$ peak in the Velleda and Grindstone Members at the western exposures of the Ellis Bay Formation (Long, 1993) may correspond to the initial rise in the $\delta^{13}C$ record of the Hirnantian excursion, and the $\delta^{13}C_{carb}$ peak in the Laframboise Member may correlate with the second rise in the Hirnantian excursion, a viewpoint also expressed by Desrochers et al. (2010) and Achab et al. (2010). In this framework, the entire Ellis Bay Formation represents the most expanded section of Hirnantian stratigraphy in the world, with tens of meters of strata having $\delta^{13}C_{carb}$ of 0‰ separating two Hirnantian $\delta^{13}C_{carb}$ maxima. The underlying Katian and overlying Llandovery sections on Anticosti Island are in fact extremely thick. However, there are no documented Hirnantian records anywhere else in the world for which $\delta^{13}C$ returns to baseline in

Figure 12. East-west geographic δ¹³C$_{carb}$ gradients in key lithological transitions of the upper Ellis Bay and lower Becscie formations. (A) δ¹³C$_{carb}$ values of basal oncolite platform bed (Laframboise Member) increase from west to east on the rising limb of the Hirnantian δ¹³C$_{carb}$ excursion, indicating that the oncolite platform bed is time transgressive. (B) δ¹³C$_{carb}$ values of first skeletal grainstones of the Fox Point Member (Becscie Formation) decrease from east to west on the descending limb of the Hirnantian δ¹³C$_{carb}$ excursion, indicating that this unit of the Fox Point Member is time transgressive.
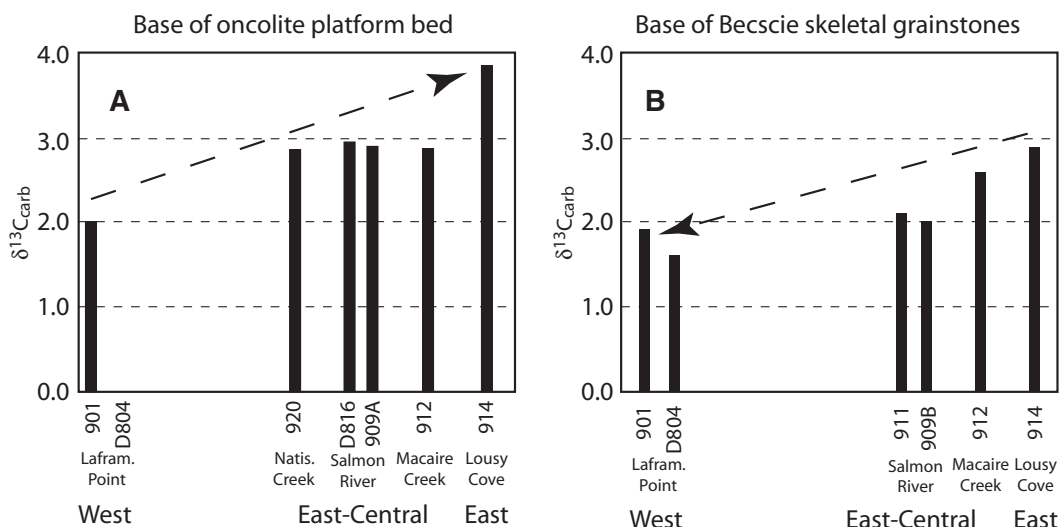
the middle of the excursion, which would be the case on Anticosti Island if the entire Ellis Bay Formation were Hirnantian.

Recently, Achab et al. (2010) presented new chitinozoan records from Anticosti and used them to argue for a thick Hirnantian section extending down to the base of the Ellis Bay Formation on the west coast. Achab et al. (2010) documented the succession of four chitinozoan biozones throughout Anticosti strata—*Herco-chitina crickmayi*, *Belonechitina gamachiana*, *Spinachitina taugourdeaui*, and *Ancyrochitina ellisbayensis*. The *H. crickmayi* zone is present throughout the upper Vauréal Formation. On the west coast, the succeeding *B. gamachiana* zone extends from the bottom of the Ellis Bay Formation through a level 1 m below the top of the bioturbated mudstones of the Lousy Cove Member. The remainder of the Lousy Cove Member belongs to the *S. taugourdeaui* zone. The Laframboise Member is devoid of chitinozoans, but the overlying Fox Point Member contains chitinozoans indicative of the *A. ellisbayensis* zone.

The chitinozoan biozones vary in their utility for global correlation among carbonate-dominated successions. Achab et al. (2010) correlated the *H. crickmayi* biozone with the *Dicellograptus anceps* graptolite zone, which is generally accepted to be of Katian age. *B. gamachiana* occurs in the Katian-aged upper Pirgu Stage of Estonia (Brenchley et al., 2003; Kaljo et al., 2008), directly underlying the Hirnantian-aged Porkuni Stage. This argues for a Katian age for the *B. gamachiana* zone (Brenchley et al., 2003; Kaljo et al., 2008; but see arguments of Achab et al., 2010). The Porkuni Stage contains an unambiguous

Hirnantian brachiopod fauna and hosts the start of the Hirnantian carbon isotope excursion and is equivalent to the *S. taugourdeaui* zone.

As pointed out by Achab et al. (2010, p. 193), "the age of the *B. gamachiana* zone is...difficult to establish and can only be inferred." This inference was achieved by noting that the chitinozoan species *Tanuchitina laurentiana* has been found in association with both *B. gamachiana* in the middle Ellis Bay Formation and with *H. crickmayi* in the upper Vauréal Formation (which is demonstrably of Katian age). The range of *T. laurentiana* in the Vinnini Formation (Nevada) begins in the Katian *Dicellograptus ornatus* zone, where it is observed to occur with *H. crickmayi*; it extends into the Hirnantian *N. extraordinarius* zone. *B. gamachiana* is absent from the Vinnini Formation (as it is from the rest of Laurentia). Because the Ellis Bay samples that contain *T. laurentiana* lack *H. crickmayi*, Achab et al. (2010) suggested that the middle Ellis Bay Formation could be of early Hirnantian age. This argument requires the absence of *B. gamachiana* in the Vinnini Formation to be insignificant, but it requires the absence of *H. crickmayi* in the Ellis Bay Formation to be highly significant. Furthermore, even if the *B. gamachiana* zone on Anticosti could be correlated with confidence to the range of *T. laurentiana* above the *D. ornatus* graptolite zone in Nevada, that still would leave the Katian-aged *Pacificograptus pacificus* graptolite zone as a viable correlative. For these reasons, we do not find the argument assigning the *B. gamachiana* zone to the Hirnantian Stage to be compelling, and therefore do not believe that existing chitino-

zoan biostratigraphy can accurately identify the Hirnantian Stage on Anticosti Island.

The shape of the δ¹³C$_{carb}$ excursion within the Laframboise Member at Laframboise Point matches the architecture of the records from the GSSPs at Dob's Linn and Wangjiawan Riverside (Fig. 3). Although previous workers did not find this to be a compelling match (Fan et al., 2009; Melchin and Holmden, 2006), they were working with the limited data set of Long (1993). The higher-resolution data presented here makes the comparison clearer. In the western sector at Laframboise Point (sections D804 and 901; Fig. 7), the excursion begins below the oncolite platform bed, in the uppermost beds of the Lousy Cove Member (Facies 6 and 7 of Desrochers et al., 2010). In these beds, δ¹³C$_{carb}$ shifts from pre-excursion baseline to ~+2‰. A discontinuous shift upward occurs across the contact with the oncolite platform bed at the base of the Laframboise Member, after which δ¹³C$_{carb}$ ascends steeply to its maximum values. The excursion returns to baseline across a thin portion of the stratigraphy at the Laframboise–Fox Point transition. This overall pattern is the same as that seen in the complete Hirnantian sections in China and Scotland (Fig. 3). We therefore place the base of the Hirnantian Stage at Laframboise Point at the transition within the Lousy Cove Member between the nodular mudstones and the overlying grainstones and calcisiltites, ~3 m below the oncolite platform bed.

There are additional positive δ¹³C$_{carb}$ peaks lower in the stratigraphy. A small δ¹³C$_{carb}$ peak (+~2‰) is recorded ~20 m below the Laframboise Member in the east-central sector (Salmon River downstream, section D814; Fig. 8) and

~50 m below the Laframboise Member in the western sector (Junction Cliff, section D801; Fig. 13). As demonstrated by Desrochers et al. (2010) and Achab et al. (2010) and confirmed here, lithofacies are diachronous across the island, making it conceivable that these two +2‰ excursions are the same event. We suggest that this excursion is Katian (pre-Hirnantian) and may correlate with the pre-Hirnantian Paroveja excursion in Baltica (Ainsaar et al., 2010).

There is chemostratigraphic evidence for the entire Hirnantian $\delta^{13}C$ excursion in the uppermost Lousy Cove Member and Laframboise Member, extending into the lower Fox Point Member, and at least one separate $\delta^{13}C_{carb}$ peak lower in the pre-Hirnantian portion of the Ellis Bay Formation. Comparing these data with the global $\delta^{13}C$ database for the Upper Ordovician, we conclude that the base of the Ellis Bay Formation should be placed in the Katian Stage, perhaps near the K2-K3 boundary (Bergström et al., 2009, 2010; Ainsaar et al., 2010). This interpretation is at odds with interpretations of Anticosti Island stratigraphy that place the base of the Hirnantian Stage at the bottom of the Ellis Bay Formation based on the brachiopod (Copper, 2001; Jin and Copper, 2008), graptolite (Melchin, 2008), and chitinozoan (Achab et al., 2010) biostratigraphy.

Deposition of the Oncolite Platform Bed

The oncolite platform bed (Petryk, 1981) is a marker bed defining the base of the Laframboise Member (Long and Copper, 1987a). It was identified in all measured sections of the Laframboise Member. We find significant stepwise discontinuities in the $\delta^{13}C_{carb}$ measurements across the base of the oncolite at all sections examined in the east-central and eastern sectors, but not in the west (Table 2). This is chemostratigraphic evidence for a significant hiatus or erosional truncation at the base of the oncolite platform bed in the more nearshore sections. The base of the oncolite bed fills in an eroded and pitted surface with up to 10 cm of local relief, providing sedimentological evidence for discontinuous accumulation in all measured sections, although the $\delta^{13}C_{carb}$ continuity in the western sector suggests that not much time is missing there. We can use the absolute values of the $\delta^{13}C_{carb}$ measurements of the base of the oncolite bed to track the timing of the deposition of this unique facies. Using the ascending limb of the positive carbon isotope excursion as a time line (Brenchley et al., 2003), it appears that the oncolite bed was deposited earlier in the western sector (where average $\delta^{13}C_{carb}$ of the oncolite is 2.0‰) than in the east-central sector (where average $\delta^{13}C_{carb}$ of the oncolite is

~2.9‰). In the eastern sector, the oncolite constitutes the entirety of the Laframboise Member, and $\delta^{13}C_{carb}$ begins at 3.7‰. Brenchley et al. (2003) pointed out that the Hirnantian positive carbon isotope excursion can be used as a "ruler" against which the rapid environmental changes of the Late Ordovician can be ordered. Brenchley et al. (2003) used the excursion to achieve high-resolution stratigraphic correlations between Laurentia and Baltica; we use it to achieve high-resolution basin-scale correlations within the Anticosti Basin. Using the ascending limb of the excursion as a time-varying signal, we infer that deposition of the oncolite platform bed was diachronous, progressing from west to east, as would be expected on a west-dipping platform during a transgression.

The character of the deposits directly underlying the oncolite platform beds is markedly different in the eastern sector compared to the rest of the island. There are no sub-oncolite grainstones in the uppermost Lousy Cove Member of the eastern sector. The mudstones that directly underlie the oncolite have $\delta^{13}C_{carb}$ values of ~0.5‰, whereas the sub-oncolitic grainstones in the other sectors have $\delta^{13}C_{carb}$ values of ~2.0‰. These observations suggest that the uppermost beds of the Lousy Cove Member in the eastern sector are older than rocks that occupy the same stratigraphic position in the east-central and western sectors. We infer geographic variations in the amount of erosion that occurred during the hiatus, with less of the underlying Lousy Cove Member preserved in the far east. Precise stratigraphic correlation of the sub-oncolitic Lousy Cove Member across the island is critical to the correct placement of biostratigraphically useful fossils and the interpretation of first and last appearances of taxa during the end-Ordovician extinctions.

Ellis Bay–Becscie Contact and the Ordovician-Silurian Boundary

The Ellis Bay–Becscie contact has been suggested to represent the Ordovician-Silurian boundary (Cocks and Copper, 1981; Nowlan, 1982; Long and Copper, 1987a; Soufiane and Achab, 2000; Copper, 2006; Melchin, 2008), but the Ordovician-Silurian boundary has also been placed within the lower several meters of the Becscie Formation (McCracken and Barnes, 1981; Petryk, 1981; Copper, 1999; Desrochers et al., 2010). As described already, in the west, the basal Becscie Formation records a quick return in $\delta^{13}C_{carb}$ to its pre-excursion 0‰ baseline following the Hirnantian positive excursion. The $\delta^{13}C_{carb}$ values in the lower Becscie of the east-central and eastern sectors stays elevated at +2‰ for at least 10 m above the Laframboise Member.

The $\delta^{13}C_{carb}$ chemostratigraphy suggests that the Ellis Bay–Becscie contact is time transgressive across the island; the lithostratigraphic boundary should not be taken as a chronostratigraphic boundary. Because diagnostic graptolites, conodonts, and chitinozoans cannot precisely pin the base of the Silurian on Anticosti Island, and because lithofacies are diachronous across the island, we suggest the use of the $\delta^{13}C_{carb}$ curve as an aid for identifying the Ordovician-Silurian boundary. The isotope curves from the Hirnantian and Silurian GSSPs (Fig. 3) show that following the Hirnantian excursion, $\delta^{13}C_{org}$ returned to baseline at the Ordovician-Silurian boundary. Therefore, chemostratigraphic correlation suggests that the Ordovician-Silurian boundary on Anticosti Island is located in the lower Becscie Formation (Achab et al., 2010). Our results demonstrate that this chemostratigraphic marker occurs at different levels within the Becscie Formation and is dependent upon geography; the Ordovician-Silurian boundary is 1–2 m above the Ellis Bay–Becscie contact in the west and ~20 m above the contact at Salmon River. We did not recover a return to isotopic baseline in our sampling of the eastern sector.

A SEQUENCE-STRATIGRAPHIC FRAMEWORK FOR THE DEPOSITION OF THE LAFRAMBOISE MEMBER

Using lithostratigraphy and biostratigraphy, Desrochers et al. (2010) presented a sequence-stratigraphic model for the entire Ellis Bay Formation and identified five transgressive-regressive (TR) cycles, with the Laframboise Member identified as the fifth cycle (TR-5). Desrochers et al. (2010) showed that sedimentation during TR-1 through TR-4 was diachronous across the basin, challenging the east-west correlations proposed by Long and Copper (1987a). For example, the time line represented by the TR-1–TR-2 boundary occurs in the Grindstone Member in the western sector, but it occurs in the Lousy Cove Member in the eastern sector. Diachroneity of facies is also supported by chitinozoan biostratigraphy (Achab et al., 2010); the boundary between the *H. crickmayi* and *B. gamachiana* biozones occurs in the Grindstone Member in the west and in the Lousy Cove Member in the east.

The high-resolution chemostratigraphic data presented here provide a means of intrabasinal correlation that exceeds the resolution available through lithostratigraphy and biostratigraphy. In this section, we use the ascending and descending limbs of the positive $\delta^{13}C_{carb}$ excursion as a chronometer to construct a chronology of individual rock units for all the measured sections of the Laframboise Member. We seek to use the

Figure 13. Composite $\delta^{13}C_{carb}$ data from multiple measured sections of outcrops from English Head to Laframboise Point and Cape Henri, western Anticosti Island. Data are from sections D821, D801–D806, and 901. See Figure 1 for section locations and Figure 8 for legend. Filled data points are from Ellis Bay Formation; open data points are from Becscie Formation. Member boundaries below the Laframboise Member have not been formalized on the west coast and are used here informally. LFB—Laframboise Member, VPDB—Vienna Peedee belemnite.
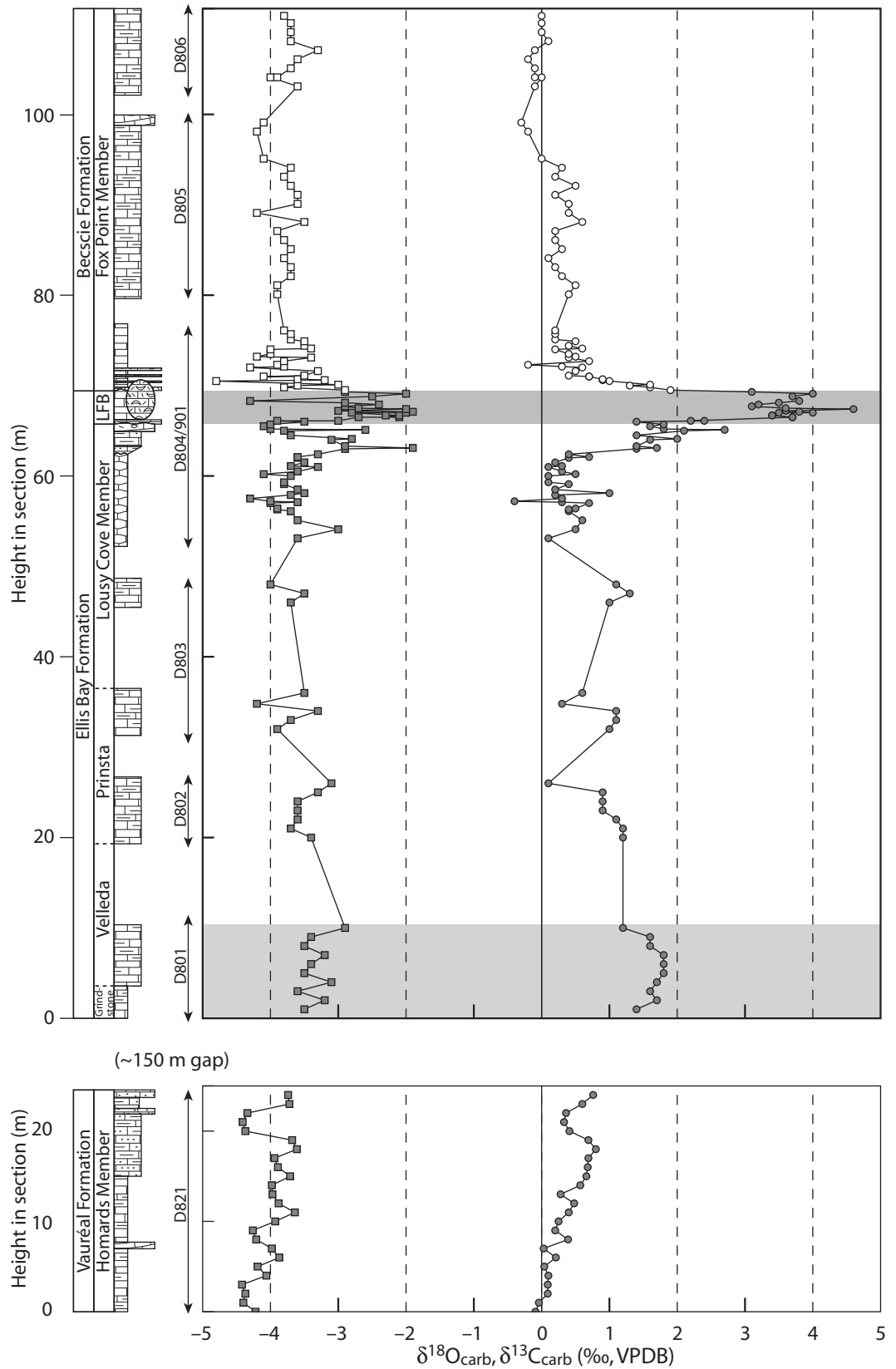
TABLE 2. SUMMARY OF $\delta^{13}C_{carb}$ DATA ACROSS THE LOUSY COVE–LAFRAMBOISE
CONTACT, INDICATING A DISCONFORMITY AT THE CONTACT

Section	Uppermost Lousy Cove Member (‰, VPDB)	Base of Laframboise Member oncolite (‰, VPDB)	Difference (‰, VPDB)
901/D804	1.8	2.2	0.4
920	1.9	2.9	1.0
D816	1.9	2.9	1.0
909A	2.0	2.9	1.0
909B	2.1	2.9	0.8
912A	2.2	2.9	0.7
914A	0.5	2.4	1.9
914B	0.5	3.8	3.3

Note: VPDB—Vienna Peedee belemnite.

improved temporal resolution available through chemostratigraphy to develop a more detailed model for the deposition of the Lousy Cove, Laframboise, and Fox Point Members and in doing so refine the chronology of glacioeustatic sea-level change, carbon cycle perturbation, and extinction.

Disconformities in the succession are observable at the outcrop scale, and we can confirm their locations by identifying discontinuities in $\delta^{13}C_{carb}$ across the unconformable surfaces. The surface separating the top of the Lousy Cove mudstones from the sandy carbonate grainstones (in the west and east-central sectors) or the oncolite platform bed (in the east sector) is one disconformity. In addition, the base of the oncolite platform bed in the Laframboise Member and the base of the Fox Point Member were previously identified as disconformities (Brenchley et al., 2003; Bergström et al., 2006; Desrochers et al., 2010). However, the nature of these disconformities is variable across the island. The $\delta^{13}C_{carb}$ data show a relatively small discontinuity across the sub-oncolitic surface in the west, a moderate increase in the east-central region, and a large step function in the east. A nearly opposite geographic pattern is identified at the base of the Becscie Formation; the $\delta^{13}C_{carb}$ discontinuity across the Ellis Bay–Becscie contact is nonexistent or very small in the east and grows in magnitude in the east-central sections. At the westernmost section, high-resolution sampling and chemostratigraphy demonstrate that there is not a large hiatus at the formation boundary; the surface separating the Laframboise Member from the Fox Point Member does not represent a profound unconformity, but rather a submarine hardground related to sediment starvation.

Because the positive $\delta^{13}C_{carb}$ excursion is a time-varying signal, we use it as a proxy for time. Scaling the lithostratigraphy against $\delta^{13}C_{carb}$ distributes individual packages of rock in time (vertical dimension of Fig. 14). Plotting the scaled measured sections as a function of east-west location on the island reinforces the trends identified in Figure 12 and yields a chronostratigraphic diagram with high temporal resolution (Fig. 14). The vertical scale in Figure 14 is constructed linearly for clarity, but we note that the rate of change of $\delta^{13}C_{carb}$ was probably variable with time. The chronostratigraphic diagram provides a basis for developing a sequence-stratigraphic model for deposition of the Lousy Cove, Laframboise, and Fox Point Members. Because the Anticosti Basin carbonate ramp dipped to the west, changes in sea level correspond to migration of facies belts in an east-west direction.

The Lousy Cover Member was deposited under relatively deep waters in all parts of the island during the highstand systems tract (HST), and we identify the disconformity at the top of the Lousy Cove Member mudstones as the sequence boundary (SB) of a depositional sequence. This is the surface representing the start of sea-level fall, above which the falling stage systems tract (FSST) and/or lowstand systems tract (LST) developed. During sea-level fall, increased erosion and siliciclastic input can generate a disconformable surface topped by reworked sediment; this is our interpretation of the cross-bedded sandy carbonate grainstone package that separates the Lousy Cove mudstones from the oncolite platform bed in the western and east-central sectors (Fig. 14). The FSST/LST is completely absent in the eastern sector, probably due to subaerial exposure and erosion.

The chronostratigraphic diagram shows that the oncolite platform bed was deposited diachronously, with deposition beginning in the west and proceeding to the east. This temporal pattern is likely the result of rising sea-level transgressing up the carbonate ramp from the more distal western end to the more proximal eastern end. We identify the base of the oldest oncolite (in the western sector) as the transgressive surface (TS) that marks the beginning of the transgressive systems tract (TST). The hiatus below the oncolite platform bed in the east-central and eastern sectors is likely the result of transgressive ravinement as the shoreline moved up the ramp, and the oncolite plat-

form bed itself is a transgressive lag deposit. Desrochers et al. (2010) also viewed the oncolite as a transgressive lag.

The Laframboise Member above the transgressive surface and, in the east-central sector, the resistant sandstones of the lowermost Fox Point Member together comprise the transgressive systems tract (TST). The isotope record at the sandstone-grainstone contact within the lower Fox Point Member shows a sharp discontinuity in $\delta^{13}C_{carb}$ in the east-central sector, indicating a brief period of nondeposition in these sections, perhaps due to carbonate sediment starvation as sea level rose rapidly. Deposition of the Fox Point sandstones ended diachronously within the east-central sector, occurring first in the westernmost section (Salmon River upstream) and last in the easternmost section (Macaire Creek), supporting a sediment starvation hypothesis for the hiatus. In the far western sector, at Laframboise Point, $\delta^{13}C_{carb}$ stratigraphy indicates that a highly condensed sedimentary package was deposited with the bioherms. In this deeper, more distal location, slow in situ carbonate production in relatively calm waters may have facilitated the accumulation of this fairly complete condensed section. This interpretation of the western sector contact between the Laframboise and Fox Point Members contrasts with that of Desrochers et al. (2010), who favored an exposure surface and meters of erosion. Because we observe an interfingering relationship between the top of the bioherms and the oldest Becscie grainstones (Fig. 4F), we conclude that sedimentation was continuous, though very slow, in this location. Other than the slow growth of the bioherms, the west was sediment starved until the prograding Fox Point Member provided additional sediment, as discussed later herein. This interval of sediment starvation may have produced the hardground surface capping the Laframboise Member at Laframboise Point that Desrochers et al. (2010) cited as evidence for subaerial exposure. Sediment starvation and hardground development at the distal western section are consistent with maximum flooding conditions during this interval.

Carbon isotope stratigraphy demonstrates that the base of the skeletal grainstones of the lower Fox Point Member is diachronous across Anticosti Island, with deposition beginning in the east and progressing westward over time (Fig. 14). We interpret the base of the Becscie Formation in the eastern sector as the maximum flooding surface (MFS), the point at which sediment accumulation began to outpace increase in sea-level rise. Sediments therefore prograded out across the ramp, filling in the proximal basin first and the more distal parts of the basin later.
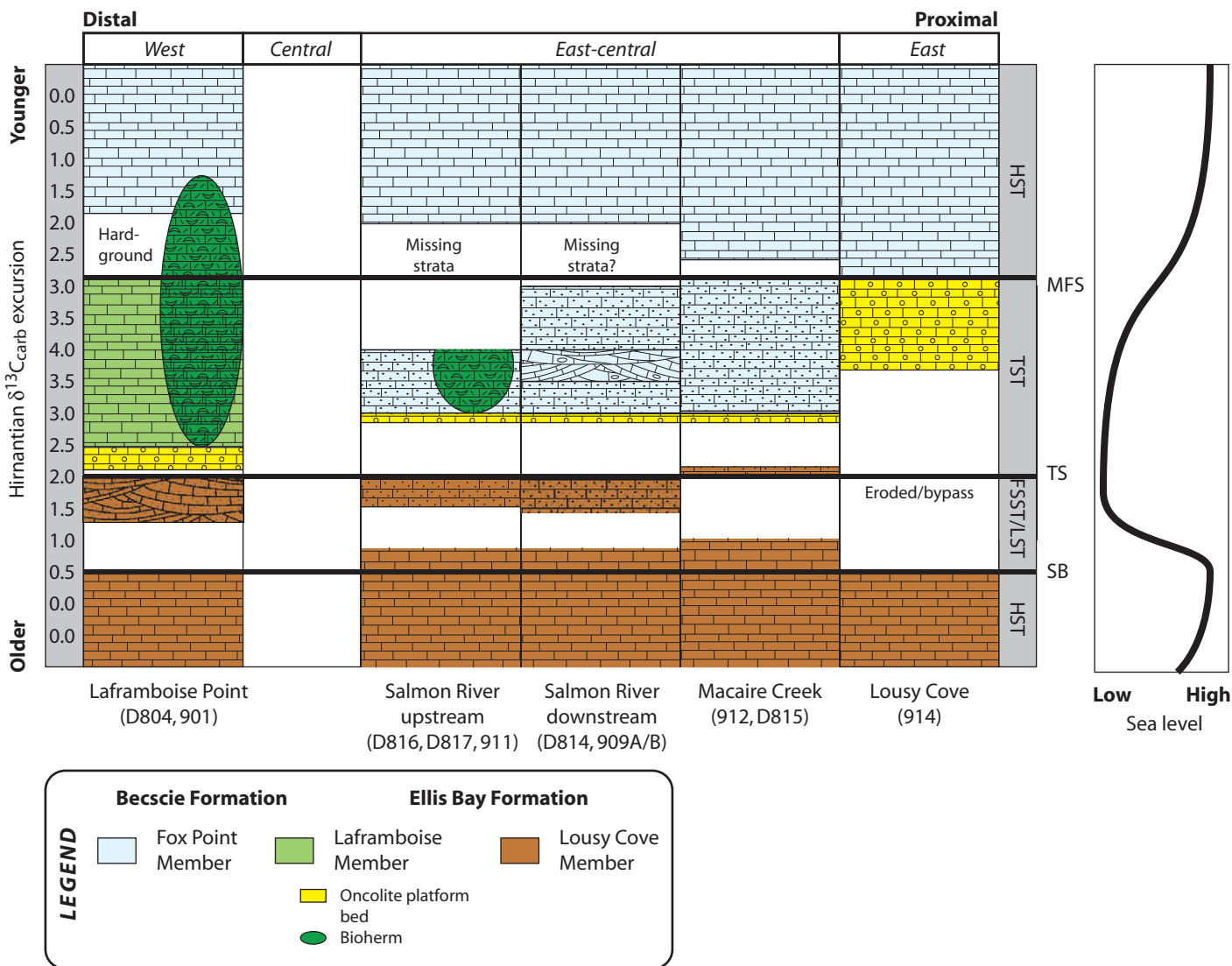
Figure 14. Chronostratigraphic diagram of upper Lousy Cove, Laframboise, and Lower Fox Point Members based on $\delta^{13}C_{carb}$ stratigraphy at five sections in an east-west transect of Anticosti Island. Vertical axis is $\delta^{13}C_{carb}$ (‰) during the Hirnantian positive isotope excursion. Although the vertical axis has been plotted on a linear scale, subdivisions in the isotope axis probably do not represent equal intervals of time. There are no adequate outcrop exposures for data in the central portion of the island. SB—sequence boundary, TS—transgressive surface, MFS—maximum flooding surface, HST—highstand systems tract, FSST—falling stage systems tract, LST—lowstand systems tract, TST—transgressive systems tract.

As such, the bulk of the Fox Point Member represents the highstand systems tract (HST) of the depositional sequence.

The sequence-stratigraphic model outlined here, based on integrated lithostratigraphy and carbon isotope chemostratigraphy, implies that maximum glacioeustatic sea-level fall occurred at the top of the Lousy Cove mudstones, and that sea level was rising during the deposition of the Laframboise and Fox Point Members. The consequences of this interpretation for end-Ordovician Earth history are developed in the next section.

IMPLICATIONS FOR THE PLACEMENT OF THE ORDOVICIAN-SILURIAN BOUNDARY AND INTERPRETATION OF LINKAGES AMONG GLACIATION, ISOTOPE EXCURSIONS, AND MASS EXTINCTION

The integrated sequence-stratigraphic and chemostratigraphic framework presented here provides new constraints on end-Ordovician history. The relative timing of the glacioeustatic sea-level changes and the initiation and termination of the $\delta^{13}C$ excursion allow us to make infer-

ences about the cause of the isotope excursion. Furthermore, our sequence-stratigraphic model implies that similar facies in different sectors of the island are not chronostratigraphic equivalents, especially in the strata adjacent to and within the Laframboise Member. This observation has bearing on the temporal distribution of first and last appearances of fossils in the basin, and therefore may complicate interpretations of the end-Ordovician mass extinction on Anticosti Island. The base of the Silurian at Dob's Linn is isotopically characterized by $\delta^{13}C_{org}$ values at pre-excursion baseline. The excursion is

over by the start of the Silurian. Our data therefore imply that, from the standpoint of isotope stratigraphy, the Ordovician-Silurian boundary is at the Ellis Bay–Becscie contact only in the westernmost sections at Laframboise Point. Farther to the east, $\delta^{13}C_{carb}$ and $\delta^{13}C_{org}$ values are elevated above baseline levels in the lower exposures of the Fox Point Member of the Becscie Formation, a consequence of the diachronous deposition during the basinward progradation of the Fox Point Member.

We infer that the forced regression during the falling stage systems tract was a response to glacioeustatic sea-level drawdown due to development of maximum glacial condition on Gondwana, and the sea-level rise associated with the transgressive systems tract was caused by melting back of the Gondwana glaciers (Fig. 14). As established by Desrochers et al. (2010), Anticosti Island records five transgressive-regressive sequences throughout the Ellis Bay Formation. Desrochers et al. (2010) interpreted the first four TR cycles as ~400 k.y. eccentricity-controlled glacial cycles and suggested that the fifth TR cycle, corresponding to the Laframboise Member, was deposited during a brief interglacial period. Our model offers an alternate interpretation for the most severe glacioeustatic sea-level change in the Ellis Bay Formation (TR-5 of Desrochers et al., 2010), associated with the Laframboise Member. We suggest that what makes the Laframboise Member lithologically distinctive is the unique environment of its deposition: the reflooding of the Anticosti Basin during terminal Ordovician deglaciation.

Published studies of carbon and oxygen isotopes from carbonate rocks on Anticosti Island (Orth et al., 1986; Long, 1993; Brenchley et al., 1994) have identified enriched $\delta^{18}O_{carb}$ and $\delta^{13}C_{carb}$ in the Laframboise Member of the Ellis Bay Formation. The oxygen data have been interpreted to represent a combination of cooling ocean temperatures and continental ice-sheet growth associated with terminal Ordovician glaciation on Gondwana (Marshall and Middleton, 1990; Long, 1993; Brenchley and Marshall, 1999; Brenchley et al., 2003). The synchrony of the $\delta^{18}O_{carb}$ and $\delta^{13}C_{carb}$ excursions has led to hypotheses linking climate change and positive carbon isotope excursions. Foremost among the competing models are the "productivity" and "weathering" hypotheses, and we next discuss these hypotheses in the context of our observations of Anticosti stratigraphy.

The "productivity" hypothesis (Marshall and Middleton, 1990; Brenchley et al., 1994) posits an increase in F_{org} (the magnitude of the total organic carbon burial flux). This has two direct effects (Kump and Arthur, 1999). First, it raises f_{org} (the fraction of total carbon buried that is organic carbon) and leads to elevated $\delta^{13}C_{carb}$ values. Second, increased F_{org} results in a drawdown of pCO_2 due to increased carbon fixation. This drop in pCO_2 is, in turn, the proposed driver for Hirnantian glaciation in this scenario (Marshall and Middleton, 1990; Brenchley et al., 1994). The productivity hypothesis does not address the ultimate cause of the proposed increase in F_{org}. Based on the relationship between pCO_2 and ice volume in the Pleistocene, it is possible that a change in pCO_2 was driven by changing ocean circulation associated with the onset or termination of glacial conditions (i.e., pCO_2 driven by glacial changes rather than vice versa). Given that we still lack a clear understanding of the causal relationship between pCO_2 and ice volume during the Pleistocene (Sigman and Boyle, 2000), it is likely that any relationship between pCO_2 and glaciation is complicated and particularly difficult to reconstruct without a robust paleo-pCO_2 proxy. We note that $\Delta^{13}C$ has been proposed as a proxy for reconstructing paleo-pCO_2 (Arthur et al., 1985; Popp et al., 1989; Laws et al., 1995). However, no substantive reproducible change in $\Delta^{13}C$ is found in our data, nor in the majority of Hirnantian chemostratigraphic studies (e.g., LaPorte et al., 2009; but see Young et al. [2010] for an alternate view). Further, $\Delta^{13}C$ is believed to reflect many other parameters and, as such, does not constitute a robust pCO_2 indicator. This leads us to conclude that a complex set of factors was controlling $\Delta^{13}C$ on a spatial scale much smaller than the size of the Anticosti Basin. We do not make any global scale inferences from the $\Delta^{13}C$ data and caution against such speculation in studies that do not reproduce $\Delta^{13}C$ signals from multiple locations within a basin. In summary, there is no firm geochemical evidence based on Anticosti $\Delta^{13}C$ for a decrease in pCO_2 associated with the Hirnantian glaciation and $\delta^{13}C$ excursion. On the other hand, an increase in f_{org} remains consistent with the observed $\delta^{13}C_{carb}$ and $\delta^{13}C_{org}$ data presented here and reported elsewhere.

The "weathering" hypothesis (Kump et al., 1999; Melchin and Holmden, 2006) was originally formulated to explain the aforementioned positive $\Delta^{13}C$ coincident with the $\delta^{13}C_{carb}$ excursion observed in Monitor Range, Nevada. In this scenario, atmospheric pCO_2 is thought to have decreased leading into the glaciations, and the subsequent $\Delta^{13}C$ excursion is interpreted as evidence of increasing pCO_2 due to reduced silicate weathering during the time that continental ice was covering silicate rock terranes during glaciation until greenhouse forcing crossed a threshold needed to deglaciate Gondwana. Kump et al. (1999) posited that pCO_2 increased over the course of the glaciation until greenhouse forcing crossed the pCO_2 threshold needed to deglaciate Gondwana. As mentioned already, there is no support for a substantive reproducible change in $\Delta^{13}C$ in our Anticosti data and, as such, no geochemical evidence for an increase in pCO_2 spanning the Hirnantian glaciation and $\delta^{13}C$ excursion.

The "weathering" hypothesis (Kump et al., 1999; Melchin and Holmden, 2006) also provides a separate explanation for the cause of the $\delta^{13}C_{carb}$ excursion. In this scenario, the positive $\delta^{13}C_{carb}$ excursion is due to the enhanced weathering of freshly exposed carbonate rocks during glacioeustatic sea-level fall. Isotope mass balance models (Kump et al., 1999; Kump and Arthur, 1999) show that $\delta^{13}C_{carb}$ rises if the freshly exposed material has a higher ratio of carbonate carbon to organic carbon than what was weathering previously. As such, Hirnantian glacioeustatic sea-level fall would have resulted in an increase in the $\delta^{13}C$ composition of the riverine input to the oceans. This explanation for the $\delta^{13}C_{carb}$ excursion does not require any change in f_{org}, the organic carbon burial fraction. An increase in riverine $\delta^{13}C$ is consistent with the observed $\delta^{13}C_{carb}$ and $\delta^{13}C_{org}$ data presented here and reported elsewhere.

We are left with two contrasting explanations for the origin of the Hirnantian $\delta^{13}C$ excursion, one due to increased organic carbon burial (Marshall and Middleton, 1990; Brenchley et al., 1994) and the other due to increased $\delta^{13}C$ of riverine input (Kump et al., 1999). Both of these scenarios result in parallel increases in $\delta^{13}C_{carb}$ and $\delta^{13}C_{org}$, and our paired geochemical data on their own cannot discriminate between them.

It is possible, however, to use the relationship between the carbon isotopic excursion and our reconstructed sea-level curve to further constrain possible mechanisms for generating the Hirnantian $\delta^{13}C$ excursion. The identification of the beginning and end of the maximal pulse of end-Ordovician glaciation in the Anticosti stratigraphic record allows us to determine the relative timing of the carbon isotope excursion and the culmination of the ice age. On Anticosti, the start of the ascending limb of the $\delta^{13}C$ excursion coincides with the sequence boundary at the top of the Lousy Cove Member (Fig. 14). The "productivity hypothesis" (Marshall and Middleton, 1990; Brenchley et al., 1994; Marshall et al., 1997) predicts that increased carbon burial lowered pCO_2 until a climatic threshold was crossed that allowed polar glaciers to develop. At the resolution provided by sequence stratigraphy and chemostratigraphy, we see no evidence for an increase in organic carbon burial (as indicated by a positive $\delta^{13}C$ excursion) before the initiation of maximum continental ice-sheet growth and glacioeustatic sea-level fall.

Our interpretation of the paired sequence-stratigraphic and carbon isotope data also implies that the $\delta^{13}C$ excursion peaked during maximum glacial conditions and that (deglacial) sea-level rise had begun before the $\delta^{13}C$ excursion ended. The maximum flooding surface occurs when $\delta^{13}C_{carb}$ is ~3‰, on the descending limb of the excursion (Fig. 14). This relative timing is consistent with the two aforementioned mechanisms for increased $\delta^{13}C$ during the Hirnantian: elevated f_{org} (Brenchley et al., 1994) and increased $\delta^{13}C$ of riverine input (Kump et al., 1999), allowing for the time lag corresponding to a change in carbon cycling to propagate through the ocean system (Kump and Arthur, 1999). The constraints on the timing of latest Ordovician glacioeustatic sea-level changes provided here may provide new insights for future modeling efforts focused on the origin of the Hirnantian positive carbon isotope excursion.

CONCLUSIONS

Our stratigraphic and isotopic studies of the carbonate rocks spanning the Ordovician-Silurian boundary across Anticosti Island suggest the following.

The globally documented positive carbon isotope excursion during the Hirnantian Stage is recorded in both carbonate and organic carbon at the Ellis Bay–Becscie contact. The magnitude of the excursion is ~3‰–4‰ in both phases.

Detailed chemostratigraphy of the upper Vauréal and the Ellis Bay Formations reveals a small positive $\delta^{13}C_{carb}$ excursion below the Laframboise Member, with tens of meters of carbonate strata at 0‰ in between. This suggests that the Laframboise–lower Fox Point Members contain a complete record of the Hirnantian Stage, and the lower $\delta^{13}C_{carb}$ peaks may correspond to a Katian excursion documented in Baltica and Laurentia.

Using the ascending limb of the $\delta^{13}C_{carb}$ excursion as a time-varying signal, we interpret the base of the oncolite platform bed (Laframboise Member, Ellis Bay Formation) to be time transgressive, with deposition progressing across the basin from west to east.

The smooth nature of the descending limb of the $\delta^{13}C_{carb}$ curve at Laframboise Point suggests that there is not a major hiatus across the Ordovician-Silurian boundary in this section.

The skeletal grainstones at the base of the Fox Point Member (Becscie Formation) are diachronous across the island, with deposition progressing from east to west. The Ordovician-Silurian boundary likely occurs tens of meters into the lower Fox Point Member in the east, and 1–2 m above the Laframboise–Fox Point contact in the west.

Integrated lithostratigraphy and isotope chemostratigraphy form the foundation of a sequence-stratigraphic model for deposition of the Laframboise Member. Glacioeustatic sea-level fall caused a forced regression that deposited the cross-stratified sand beds beneath the oncolite platform bed. Reflooding of the ramp during deglaciation led to deposition of the transgressive oncolite platform bed (transgressive lag of the transgressive systems tract) and the remainder of the Laframboise Member and lower Becscie sandstones. As sea-level rise slowed, skeletal grainstones of the Fox Point Member (highstand systems tract) prograded basinward, from east to west.

The observed relative timing between sea-level fall and the beginning of the $\delta^{13}C$ excursions is consistent with the "weathering" hypothesis advanced to explain the origin of the Hirnantian positive $\delta^{13}C_{carb}$ excursion. The excursion persisted through deglacial sea-level rise, indicating that the response time for the Hirnantian carbon cycle perturbation is discernible in the Anticosti stratigraphic record.

REFERENCES CITED

Achab, A., Asselin, E., Desrochers, A., Riva, J.F., and Farley, C., 2011, Chitinozoan contribution to the development of a new Upper Ordovician stratigraphic framework for Anticosti Island: Geological Society of America Bulletin, v. 123, p. 186–205, doi: 10.1130/B30131.1.

Ainsaar, L., Kaljo, D., Martma, T., Meidla, T., Männik, P., Nõlvak, J., and Tinn, O., 2010, Middle and Upper Ordovician carbon isotope chemostratigraphy in Baltoscandia: A correlation standard and clues to environmental history: Palaeogeography, Palaeoclimatology, Palaeoecology, v. 294, p. 189–201, doi: 10.1016/j.palaeo.2010.01.003.

Arthur, M.A., Dean, W.E., and Claypool, G.E., 1985, Anomalous ^{13}C enrichment in modern marine organic carbon: Nature, v. 315, p. 216–218, doi: 10.1038/315216a0.

Bambach, R.K., Knoll, A.H., and Wang, S.C., 2004, Origination, extinction, and mass depletions of marine diversity: Paleobiology, v. 30, p. 522–542, doi: 10.1666/0094-8373(2004)030<0522:OEAMDO>2.0.CO;2.

Banner, J.L., and Hanson, G., 1990, Calculation of simultaneous isotopic and trace element variations during water-rock interaction with applications to carbonate diagenesis: Geochimica et Cosmochimica Acta, v. 54, p. 3123–3137, doi: 10.1016/0016-7037(90)90128-8.

Barnes, C.R., 1988, Stratigraphy and palaeontology of the Ordovician-Silurian boundary interval, Anticosti Island, Québec, Canada: Bulletin of the British Museum of Natural History (Geology), v. 43, p. 195–219.

Bergström, S.M., Saltzman, M.R., and Schmitz, B., 2006, First record of the Hirnantian (Upper Ordovician) $\delta^{13}C$ excursion in the North American Midcontinent and its regional implications: Geological Magazine, v. 143, p. 657–678, doi: 10.1017/S0016756806002469.

Bergström, S.M., Chen, X., Gutierrez-Marco, J.C., and Dronov, A., 2009, The new chronostratigraphic classification of the Ordovician System and its relations to major regional series and stages and to $\delta^{13}C$ chemostratigraphy: Lethaia, v. 42, p. 97–107, doi: 10.1111/j.1502-3931.2008.00136.x.

Bergström, S.M., Young, S., and Schmitz, B., 2010, Katian (Upper Ordovician) $\delta^{13}C$ chemostratigraphy and sequence stratigraphy in the United States and Baltoscandia: A regional comparison: Palaeogeography, Palaeoclimatology, Palaeoecology, v. 296, p. 217–234, doi: 10.1016/j.palaeo.2010.02.035.

Berner, R.A., 2006, GEOCARBSULF: A combined model for Phanerozoic atmospheric O_2 and CO_2: Geochimica et Cosmochimica Acta, v. 70, p. 5653–5664, doi: 10.1016/j.gca.2005.11.032.

Bordet, E., Malo, M., and Kirkwood, D., 2010, A structural study of western Anticosti Island, St. Lawrence platform, Québec: A fracture analysis that integrates surface and subsurface structural data: Bulletin of Canadian Petroleum Geology, v. 58, p. 36–55, doi: 10.2113/gscpgbull.58.1.36.

Brenchley, P.J., and Marshall, J.D., 1999, Relative timing and critical events during the Late Ordovician mass extinction—New data from Oslo: Acta Universitatis Carolinae-Geologica, v. 43, p. 187–190.

Brenchley, P.J., Marshall, J.D., Carden, G.A.F., Robertson, D.B.R., Long, D.G.F., Meidla, T., Hints, L., and Anderson, T.F., 1994, Bathymetric and isotopic evidence for a short-lived Late Ordovician glaciation in a greenhouse period: Geology, v. 22, p. 295–298, doi: 10.1130/0091-7613(1994)022<0295:BAIEFA>2.3.CO;2.

Brenchley, P.J., Marshall, J., and Underwood, C., 2001, Do all mass extinctions represent an ecological crisis? Evidence from the Late Ordovician: Geological Journal, v. 36, p. 329–340, doi: 10.1002/gj.880.

Brenchley, P.J., Carden, G.A.F., Hints, L., Kaljo, D., Marshall, J.D., Martma, T., Meidla, T., and Nõlvak, J., 2003, High-resolution stable isotope stratigraphy of Upper Ordovician sequences: Constraints on the timing of bioevents and environmental changes associated with mass extinction and glaciation: Geological Society of America Bulletin, v. 115, p. 89–104, doi: 10.1130/0016-7606(2003)115<0089:HRSISO>2.0.CO;2.

Caputo, M.V., and Crowell, J.C., 1985, Migration of glacial centers across Gondwana during Paleozoic Era: Geological Society of America Bulletin, v. 96, p. 1020–1036, doi: 10.1130/0016-7606(1985)96<1020:MOGCAG>2.0.CO;2.

Chen, X., Rong, J., Fan, J., Zhan, R., Mitchell, C.E., Harper, D.A.T., Melchin, M.J., Peng, P., Finney, S.C., and Wang, X., 2006, The global boundary stratotype section and point (GSSP) for the base of the Hirnantian Stage (the uppermost of the Ordovician System): Episodes, v. 29, p. 183–196.

Cocks, L.R.M., and Copper, P., 1981, The Ordovician-Silurian boundary at the eastern end of Anticosti Island: Canadian Journal of Earth Sciences, v. 18, p. 1029–1034.

Copper, P., 1999, Brachiopods during and after the Late Ordovician mass extinctions, Anticosti Island, E Canada: Acta Universitatis Carolinae-Geologica, v. 43, p. 207–209.

Copper, P., 2001, Reefs during the multiple crises towards the Ordovician-Silurian boundary: Anticosti Island, eastern Canada, and worldwide: Canadian Journal

of Earth Sciences, v. 38, p. 153–171, doi: 10.1139/cjes-38-2-153.

Copper, P., 2006, Faunal change across the Ordovician-Silurian mass extinction boundary on Anticosti Island, E Canada: Geological Society of America Abstracts with Programs, v. 38, no. 7, p. 403.

Copper, P., and Long, D.G.F., 1989, Stratigraphic revisions for a key Ordovician/Silurian boundary section, Anticosti Island, Canada: Newsletters on Stratigraphy, v. 21, p. 59–73.

Delabroye, A., and Vecoli, M., 2010, The end-Ordovician glaciation and the Hirnantian Stage: A global review and questions about Late Ordovician event stratigraphy: Earth-Science Reviews, v. 98, p. 269–282, doi: 10.1016/j.earscirev.2009.10.010.

Desrochers, A., and Gauthier, E.L., 2009, Carte Géologique Synthèse de l'Île d'Anticosti. Annotated Map: Québec, Ministère des Ressources naturelles et de la Faune, scale 1:250,000.

Desrochers, A., Farley, C., Achab, A., Asselin, E., and Riva, J.F., 2010, A far-field record of the end Ordovician glaciation: The Ellis Bay Formation, Anticosti Island, Eastern Canada: Palaeogeography, Palaeoclimatology, Palaeoecology, v. 296, p. 248–263, doi: 10.1016/j.palaeo.2010.02.017.

Díaz-Martínez, E., and Grahn, Y., 2007, Early Silurian glaciation along the western margin of Gondwana (Peru, Bolivia and northern Argentina): Palaeogeographic and geodynamic setting: Palaeogeography, Palaeoclimatology, Palaeoecology, v. 245, p. 62–81, doi: 10.1016/j.palaeo.2006.02.018.

Emiliani, C., 1966, Isotopic paleotemperatures: Science, v. 154, p. 851–857, doi: 10.1126/science.154.3751.851.

Fan, J., Peng, P., and Melchin, M.J., 2009, Carbon isotopes and event stratigraphy near the Ordovician-Silurian boundary, Yichang, South China: Palaeogeography, Palaeoclimatology, Palaeoecology, v. 276, p. 160–169, doi: 10.1016/j.palaeo.2009.03.007.

Farley, C., and Desrochers, A., 2007, Sediment dynamics and stratigraphic architecture of a mixed carbonate-siliciclastic ramp: The Upper Ordovician (Hirnantian) Ellis Bay Formation, Anticosti Island, Québec, Canada: Geological Society of America Abstracts with Programs, v. 39, p. 419.

Finney, S.C., Berry, W.B.N., Cooper, J.D., Ripperdan, R.L., Sweet, W.C., Jacobson, S.R., Soufiane, A., Achab, A., and Noble, P.J., 1999, Late Ordovician mass extinction: A new perspective from stratigraphic sections in central Nevada: Geology, v. 27, p. 215–218, doi: 10.1130/0091-7613(1999)027<0215:LOMEAN>2.3.CO;2.

Ghienne, J.-F., 2003, Late Ordovician sedimentary environments, glacial cycles, and post-glacial transgression in the Taoudeni Basin, West Africa: Palaeogeography, Palaeoclimatology, Palaeoecology, v. 189, p. 117–145, doi: 10.1016/S0031-0182(02)00635-1.

Grahn, Y., and Caputo, M.V., 1992, Early Silurian glaciations in Brazil: Palaeogeography, Palaeoclimatology, Palaeoecology, v. 99, p. 9–15, doi: 10.1016/0031-0182(92)90003-N.

Hambrey, M.J., 1985, The Late Ordovician–Early Silurian glacial period: Palaeogeography, Palaeoclimatology, Palaeoecology, v. 51, p. 273–289, doi: 10.1016/0031-0182(85)90089-6.

Hambrey, M.J., and Harland, W.B., eds., 1981, Earth's Pre-Pleistocene Glacial Record: Cambridge, UK, Cambridge University Press, 1024 p.

Holland, C.H., 1985, Series and Stages of the Silurian System: Episodes, v. 8, p. 101–103.

Holmden, C.E., Creaser, R.A., Muehlenbachs, K., Leslie, S.A., and Bergström, S.M., 1998, Isotopic evidence for geochemical decoupling between ancient epeiric seas and bordering oceans: Implications for secular curves: Geology, v. 26, p. 567–570, doi: 10.1130/0091-7613(1998)026<0567:IEFGDB>2.3.CO;2.

Immenhauser, A., Porta, G.D., Kenter, J.A.M., and Bahamonde, J.R., 2003, An alternative model for positive shifts in shallow-marine carbonate $\delta^{13}C$ and $\delta^{18}O$: Sedimentology, v. 50, p. 953–959, doi: 10.1046/j.1365-3091.2003.00590.x.

Institut National de la Recherche Scientifique (INRS)-Petrole, 1974, Arco-Anticosti No. 1: Sedimentologic, mineralogical, bio-stratigraphical, geochemical, organic

and mineral study, diagenesis and petroleum potential: Sainte-Foy, Quebec, Institut National de la Recherche Scientifique, 7, 27 p.

Jin, J., and Copper, P., 2008, Response of brachiopod communities to environmental change during the Late Ordovician mass extinction interval, Anticosti Island, eastern Canada: Fossils and Strata, v. 54, p. 41–51.

Kaljo, D., Hints, L., Martma, T., and Nõlvak, J., 2001, Carbon isotope stratigraphy in the latest Ordovician of Estonia: Chemical Geology, v. 175, p. 49–59, doi: 10.1016/S0009-2541(00)00363-6.

Kaljo, D., Hints, L., Martma, T., Nõlvak, J., and Oraspld, A., 2004, Late Ordovician carbon isotope trend in Estonia, its significance in stratigraphy and environmental analysis: Palaeogeography, Palaeoclimatology, Palaeoecology, v. 210, p. 165–185, doi: 10.1016/j.palaeo.2004.02.044.

Kaljo, D., Hints, L., Maennik, P., and Nõlvak, J., 2008, The succession of Hirnantian events based on data from Baltica: Brachiopods, chitinozoans, conodonts, and carbon isotopes: Estonian Journal of Earth Science, v. 57, p. 197–218, doi: 10.3176/earth.2008.4.01.

Kamo, S.L., and Gower, C., 1994, Note: U-Pb baddeleyite dating clarifies age of characteristic paleomagnetic remanence of Long Range dykes, southeastern Labrador: Atlantic Geology, v. 30, p. 259–262.

Kump, L.R., and Arthur, M.A., 1999, Interpreting carbon-isotope excursions: Carbonates and organic matter: Chemical Geology, v. 161, p. 181–198, doi: 10.1016/S0009-2541(99)00086-8.

Kump, L.R., Arthur, M.A., Patzkowsky, M., Gibbs, M., Pinkus, D.S., and Sheehan, P.M., 1999, A weathering hypothesis for glaciation at high atmospheric pCO_2 during the Late Ordovician: Palaeogeography, Palaeoclimatology, Palaeoecology, v. 152, p. 173–187, doi: 10.1016/S0031-0182(99)00046-2.

Lake, J.H., 1981, Sedimentology and paleoecology of Upper Ordovician mounds of Anticosti Island, Québec: Canadian Journal of Earth Sciences, v. 18, p. 1562–1571.

LaPorte, D.F., Holmden, C.E., Patterson, W.P., Loxton, J.D., Melchin, M.J., Mitchell, C.E., Finney, S.C., and Sheets, H.D., 2009, Local and global perspectives on carbon and nitrogen cycling during the Hirnantian glaciation: Palaeogeography, Palaeoclimatology, Palaeoecology, v. 276, p. 182–195, doi: 10.1016/j.palaeo.2009.03.009.

Laws, E.A., Popp, B.N., Bidigare, R.R., Kennicutt, M.C., and Macko, S.A., 1995, Dependence of phytoplankton carbon isotopic composition on growth rate and $[CO_2]_{aq}$: Theoretical considerations and experimental results: Geochimica et Cosmochimica Acta, v. 59, p. 1131–1138, doi: 10.1016/0016-7037(95)00030-4.

Le Heron, D.P., and Dowdeswell, J., 2009, Calculating ice volumes and ice flux to constrain the dimensions of a 440 Ma North African ice sheet: Journal of the Geological Society of London, v. 166, p. 277–281, doi: 10.1144/0016-76492008-087.

Le Heron, D.P., and Howard, J., 2010, Evidence for Late Ordovician glaciation of Al Kufrah Basin, Libya: Journal of African Earth Sciences, v. 58, p. 354–364, doi: 10.1016/j.jafrearsci.2010.04.001.

Le Heron, D.P., Ghienne, J.-F., Houicha, M.E., Khoukhi, Y., and Rubino, J.L., 2007, Maximum extent of ice sheets in Morocco during the Late Ordovician glaciation: Palaeogeography, Palaeoclimatology, Palaeoecology, v. 245, p. 200–226, doi: 10.1016/j.palaeo.2006.02.031.

Loi, A., Ghienne, J.F., Dabard, M.P., Paris, F., Botquelen, A., Christ, N., Elaouad-Debbaj, Z., Gorini, A., Vidal, M., Videt, B., and Destombes, J., 2010, The Late Ordovician glacio-eustatic record from a high-latitude storm-dominated shelf succession (Bou Ingarf section (Anti-Atlas, southern Morocco): Palaeogeography, Palaeoclimatology, Palaeoecology, v. 296, p. 332–358, doi: 10.1016/j.palaeo.2010.01.018.

Long, D.G.F., 1993, Oxygen and carbon isotopes and event stratigraphy near the Ordovician-Silurian boundary, Anticosti Island, Québec: Palaeogeography, Palaeoclimatology, Palaeoecology, v. 104, p. 49–59, doi: 10.1016/0031-0182(93)90119-4.

Long, D.G.F., 2007, Tempestite frequency curves: A key to Late Ordovician and Early Silurian subsidence, sea-level change, and orbital forcing in the Anticosti fore-

land basin, Québec, Canada: Canadian Journal of Earth Sciences, v. 44, p. 413–431, doi: 10.1139/E06-099.

Long, D.G.F., and Copper, P., 1987a, Stratigraphy of the Upper Ordovician upper Vauréal and Ellis Bay Formations, eastern Anticosti Island, Québec: Canadian Journal of Earth Sciences, v. 24, p. 1807–1820, doi: 10.1139/e87-172.

Long, D.G.F., and Copper, P., 1987b, Late Ordovician sand-wave complexes on Anticosti Island, Québec: A marine tidal embayment?: Canadian Journal of Earth Sciences, v. 24, p. 1821–1832, doi: 10.1139/e87-173.

Marshall, J.D., and Middleton, P.D., 1990, Changes in marine isotopic composition and the late Ordovician glaciation: Journal of the Geological Society of London, v. 147, p. 1–4, doi: 10.1144/gsjgs.147.1.0001.

Marshall, J.D., Brenchley, P.J., Mason, P.R.D., Wolff, G.A., Astini, R.A., Hints, L., and Meidla, T., 1997, Global carbon isotopic events associated with mass extinction and glaciation in the Late Ordovician: Palaeogeography, Palaeoclimatology, Palaeoecology, v. 132, p. 195–210, doi: 10.1016/S0031-0182(97)00063-1.

McCracken, A.D., and Barnes, C.R., 1981, Conodont biostratigraphy and paleoecology of the Ellis Bay Formation, Anticosti Island, Québec, with special reference to Late Ordovician–Early Silurian chronostratigraphy and the systematic boundary: Geological Survey of Canada Bulletin, v. 329, p. 51–111.

Melchin, M.J., 2008, Restudy of some Ordovician-Silurian boundary graptolites from Anticosti Island, Canada, and their biostratigraphic significance: Lethaia, v. 41, p. 155–162, doi: 10.1111/j.1502-3931.2007.00045.x.

Melchin, M.J., and Holmden, C.E., 2006, Carbon isotope chemostratigraphy in Arctic Canada: Sea-level forcing of carbonate platform weathering and implications for Hirnantian global correlation: Palaeogeography, Palaeoclimatology, Palaeoecology, v. 234, p. 186–200, doi: 10.1016/j.palaeo.2005.10.009.

Melchin, M.J., and Williams, S.H., 2000, A restudy of the Akidograptine graptolites from Dob's Linn and a proposed redefined zonation of the Silurian stratotype: Palaeontology Down-Under, v. 61, p. 63.

Nowlan, G.S., 1982, Conodonts and the position of the Ordovician-Silurian boundary at the eastern end of Anticosti Island, Québec, Canada: Canadian Journal of Earth Sciences, v. 19, p. 1332–1335.

Orth, C.J., Gilmore, J.S., Quintana, L.R., and Sheehan, P.M., 1986, Terminal Ordovician extinction; geochemical analysis of the Ordovician-Silurian boundary, Anticosti Island, Québec: Geology, v. 14, p. 433–436, doi: 10.1130/0091-7613(1986)14<433:TOEGAO>2.0.CO;2.

Patterson, W., and Walter, L., 1994, Depletion of ^{13}C in seawater ΣCO_2 on modern carbonate platforms: Significance for the carbon isotopic record of carbonates: Geology, v. 22, p. 885–888, doi: 10.1130/0091-7613(1994)022<0885:DOCISC>2.3.CO;2.

Petryk, A.A., 1981, Stratigraphy, sedimentology and paleogeography of the Upper Ordovician–Lower Silurian of Anticosti Island, Québec, *in* Lesperance, P.J., ed., Subcommission on Silurian Stratigraphy, Ordovician-Silurian Working Group. Volume II: Stratigraphy and Paleontology: Anticosti-Gaspe, Québec, Universite de Montreal, p. 11–39.

Pinet, N., and Lavoie, D., 2007, The offshore part of the Anticosti Basin: A major gap in the understanding of early to middle Paleozoic basins of Eastern Canada in a promising hydrocarbon setting, *in* Convention Extended Abstracts: Calgary, Canadian Society of Petroleum and Geology, p. 336–339.

Popp, B., Takigiku, R., Hayes, J., Louda, J., and Baker, E., 1989, The post-Paleozoic chronology and mechanism for ^{13}C depletion in primary marine organic matter: American Journal of Science, v. 289, p. 436–454, doi: 10.2475/ajs.289.4.436.

Ripperdan, R.L., Cooper, J.D., and Finney, S.C., 1998, High resolution $\delta^{13}C$ and lithostratigraphic profiles from Copenhagen Canyon, Nevada: Clues to the behavior of the ocean carbon cycle during the Late Ordovician global crisis: Mineralogical Magazine, v. 62A, p. 1279–1280, doi: 10.1180/minmag.1998.62A.3.03.

Runkel, A.C., Mackey, T.J., Cowan, C.A., and Fox, D.L., 2010, Tropical shoreline ice in the Late Cambrian: Implications for Earth's climate between the Cambrian

explosion and the Great Ordovician biodiversification event: GSA Today, v. 20, no. 11, p. 4–10, doi: 10.1130/GSATG84A.1.

Sami, T., and Desrochers, A., 1992, Episodic sedimentation on an Early Silurian, storm-dominated carbonate ramp, Becscie and Merrimack Formations, Anticosti Island, Canada: Sedimentology, v. 39, p. 355–381, doi: 10.1111/j.1365-3091.1992.tb02122.x.

Sepkoski, J.J., 1981, A factor analytic description of the Phanerozoic marine fossil record: Paleobiology, v. 7, p. 36–53.

Shackleton, N.J., 1967, Oxygen isotope analyses and Pleistocene temperatures re-assessed: Nature, v. 215, p. 15–17, doi: 10.1038/215015a0.

Sheehan, P.M., 2001, The Late Ordovician mass extinction: Annual Review of Earth and Planetary Sciences, v. 29, p. 331–364, doi: 10.1146/annurev.earth.29.1.331.

Sigman, D.M., and Boyle, E.A., 2000, Glacial/interglacial variations in atmospheric carbon dioxide: Nature, v. 407, no. 6806, p. 859–869, doi: 10.1038/35038000.

Soufiane, A., and Achab, A., 2000, Chitinozoan zonation of the Late Ordovician and the Early Silurian of the Island of Anticosti, Québec, Canada: Review of Palaeobotany and Palynology, v. 109, p. 85–111, doi: 10.1016/S0034-6667(99)00044-5.

Swart, P.K., and Eberli, G.P., 2005, The nature of the $\delta^{13}C$ of periplatform sediments: Implications for stratigraphy and the global carbon cycle: Sedimentary Geology, v. 175, p. 115–129, doi: 10.1016/j.sedgeo.2004.12.029.

Underwood, C.J., Crowley, S., Marshall, J.D., and Brenchley, P.J., 1997, High-resolution carbon isotope stratigraphy of the basal Silurian stratotype (Dob's Linn, Scotland) and its global correlation: Journal of the Geological Society of London, v. 154, p. 709–718, doi: 10.1144/gsjgs.154.4.0709.

Urey, H.C., 1947, The thermodynamic properties of isotopic substances: Journal of the Chemical Society, p. 562–581.

Veizer, J., Ala, D., Azmy, K., Bruckschen, P., Buhl, D., Bruhn, F., Carden, G.A.F., Diener, A., Ebneth, S., Godderis, Y., Jasper, T., Korte, C., Pawellek, F., Podlaha, O.G., and Strauss, H., 1999, $^{87}Sr/^{86}Sr$, $\delta^{13}C$ and $\delta^{18}O$ evolution of Phanerozoic seawater: Chemical Geology, v. 161, p. 59–88, doi: 10.1016/S0009-2541(99)00081-9.

Waldron, J.W.F., Anderson, S.D., Cawood, P.A., Goodwin, L.B., Hall, J., Jamieson, R.A., Palmer, S.E., Stockmal, G.S., and Williams, P.F., 1998, Evolution of the Appalachian Laurentian margin: Lithoprobe results in western Newfoundland: Canadian Journal of Earth Sciences, v. 35, p. 1271–1287, doi: 10.1139/cjes-35-11-1271.

Wang, K., Orth, C.J., Attrep, M., Jr., Chatterton, B.D.E., Wang, X., and Li, J., 1993, The great latest Ordovician extinction on the South China plate: Chemostratigraphic studies of the Ordovician-Silurian boundary interval on the Yangtze Platform: Palaeogeography, Palaeoclimatology, Palaeoecology, v. 104, p. 61–79, doi: 10.1016/0031-0182(93)90120-8.

Wang, K., Chatterton, B.D.E., and Wang, Y., 1997, An organic carbon isotope record of Late Ordovician to Early Silurian marine sedimentary rocks, Yangtze Sea, South China: Implications for CO_2 changes during the Hirnantian glaciation: Palaeogeography, Palaeoclimatology, Palaeoecology, v. 132, p. 147–158, doi: 10.1016/S0031-0182(97)00046-1.

Webby, B.D., Paris, F., Droser, M.L., and Percival, I.G., eds., 2004, The Great Ordovician Biodiversification Event: New York, Columbia University Press, 496 p.

Yan, D., Chen, D., Wang, Q., Wang, J., and Wang, Z., 2009, Carbon and sulfur isotopic anomalies across the Ordovician-Silurian boundary on the Yangtze Platform, South China: Palaeogeography, Palaeoclimatology, Palaeoecology, v. 274, p. 32–39, doi: 10.1016/j.palaeo.2008.12.016.

Young, S.A., Saltzman, M.R., Ausich, W.I., Desrochers, A., and Kaljo, D., 2010, Did changes in atmospheric CO_2 coincide with latest Ordovician glacial-interglacial cycles?: Palaeogeography, Palaeoclimatology, Palaeoecology, v. 296, p. 376–388, doi: 10.1016/j.palaeo.2010.02.033.

Zhang, T., Shen, Y., Zhan, R., Shen, S., and Chen, X., 2009, Large perturbations of the carbon and sulfur cycle associated with the Late Ordovician mass extinction in South China: Geology, v. 37, p. 299–302, doi: 10.1130/G25477A.1.